Fottea, Olomouc, 24(1): 1–22, 2024
DOI: 10.5507/fot.2023.002

Molecular phylogenetics coupled with morphological analyses of Arctic and Antarctic strains place *Chamaepinnularia* (Bacillariophyta) within the Sellaphoraceae

Katherina Schimani[1*], Nélida Abarca[1], Jonas Zimmermann[1], Oliver Skibbe[1], Regine Jahn[1], Wolf–Henning Kusber[1], Thomas Leya[2] & Demetrio Mora[1,3]

[1] *Botanischer Garten und Botanisches Museum Berlin, Freie Universität Berlin, Königin–Luise–Straße 6–8, 14195 Berlin, Germany; *Corresponding author e–mail: k.schimani@bo.berlin*
[2] *Fraunhofer Institute for Cell Therapy and Immunology, Branch Bioanalytics and Bioprocesses (IZI–BB), Extremophile Research & Biobank CCCryo, Am Muehlenberg 13, 14476 Potsdam, Germany*
[3] *Referat U2 – Mikrobielle Ökologie, Bundesanstalt für Gewässerkunde, Am Mainzer Tor 1, 56068 Koblenz, Germany*

Abstract: The diatom genus *Chamaepinnularia* was first published by Lange–Bertalot et Krammer in 1996 to accommodate several small species previously included within *Navicula* and *Pinnularia*. Despite its morphological similarity to those two genera, the family–level classification of *Chamaepinnularia* has been considered *incertae sedis* since its description almost three decades ago. We provide the first molecular characterisation (18S and rbcL) of the genus based on cultured polar strains and investigated its phylogenetic placement. Molecular data are complemented with observations on living cells, as well as detailed examination of oxidized material with light microscopy and scanning electron microscopy. The 12 investigated strains were morphologically identified as three taxa: two already described species (*C. gerlachei*, *C. krookii*) and one here newly described (*C. australis* sp. nov.). These species formed three separate, well–supported branches in the phylogeny. Our analyses placed *Chamaepinnularia* as a sister group to members of the Sellaphoraceae for which sequence data exist (i.e. *Sellaphora*, *Fallacia*, *Rossia* and *Diprora*). Based on the presence of hymenate areolae, a single H–shaped plastid with girdle appressed plates and the results of the phylogenetic trees, we propose the inclusion of *Chamaepinnularia* within the family Sellaphoraceae, which altogether form a supported monophyletic group.

Key words: diatoms, micromorphology, molecular markers, phylogenies, polar biodiversity, unialgal cultures

Introduction

Polar regions are among the most extreme habitats on Earth, especially for photo–autotrophic organisms. The seasonal change from polar night to midnight sun is one of their hallmarks but also a distinguishing feature from all other regions on the planet. Organisms in those regions, including diatoms, must deal with extreme light and temperature regimes (Zacher et al. 2009). Despite the harsh environment, diatom biodiversity in polar regions is much more extensive, ecologically diverse, and biogeographically structured than previously thought (Vyverman et al. 2010; Pinseel et al. 2020; Verleyen et al. 2021). Despite their diversity in polar shallow–water coastal zones, benthic diatoms in this habitat are poorly known in terms of biodiversity, biogeography, and ecology. Knowledge on these phototrophs, which form a key assemblage known as microphytobenthos, stems mainly from temperate to tropical regions.

A large number of species within the genus *Chamaepinnularia* Lange–Bert. et Krammer have been described from polar habitats (Lange–Bertalot & Genkal 1999; Van de Vijver et al. 2002; Zidarova et al. 2016b) with several species endemic to the Antarctic, e.g. *C. antarctica* Van de Vijver, Kopalová, Zidarova et E.J.Cox*, C. australomediocris* (Lange–Bert. et Rol. Schmidt) Van de Vijver, *C. cymatopleura* (West et G.S.West) Cavacini*, C. elliptica* Zidarova, Kopalová et Van de Vijver*, C. gerlachei* Van de Vijver et Sterken*, C. gibsonii* Van de Vijver, and *C. gracilistriata* Van de Vijver et Beyens (Van de Vijver et al. 2002, 2010, 2012, 2013; Cavacini et al. 2006; Zidarova et al. 2016a). Additionally, two taxa were described as endemic for the Arctic and northern cold–temperate climatic zones (*C. oculus* (Østrup) Lange–Bert. in Lange–Bertalot & Genkal 1999; and *C. circumborealis* Lange–Bert. in

Lange–Bertalot & Genkal 1999; Metzeltin et al. 2009; Potapova 2014). *Chamaepinnularia* species have been found in a broad spectrum of habitats, such as aerial environments, growing as epiphytes on mosses (Van de Vijver et al. 2002, 2004; Van de Vijver & Cox 2013; Wetzel et al. 2013), springs (Werum & Lange–Bertalot 2004; Beauger et al. 2022a), hot saline springs (Wetzel & Ector 2016), freshwater lakes (Lange–Bertalot & Metzeltin 1996; Cantonati & Lange–Bertalot 2009) and marine benthic habitats (Witkowski et al. 2000).

Chamaepinnularia was first described in 1996 comprising several taxa previously classified within *Navicula* Bory and *Pinnularia* Ehrenberg, since symmetry as well as arrangement of the raphe system were not significantly different from those genera (Lange–Bertalot & Metzeltin 1996). In addition, some taxa show the typical striae–structure of *Pinnularia*–alveoli having a steep mantle. The valves of *Chamaepinnularia* species are linear, linear–elliptic to linear–lanceolate in shape with rounded or capitate apices and comparatively small sized (length < 25 µm, width < 4 µm). Distal internal raphe fissures terminate on a helictoglossa. Proximal internal raphe endings are deflected or hooked. The most distinctive feature of the genus is the ultrastructure of the stria, which consists of a single alveolus. Externally, the uniseriate striae are occluded by an unstructured hymen in proximity of the outer surface and interrupted by a hyaline area near the valve face–mantle junction (Lange–Bertalot & Metzeltin 1996; Cantonati & Lange–Bertalot 2009; Wetzel et al. 2013; Żelazna–Wieczorek & Olszyński 2016). However, this interruption seems to be variable in the genus. In *C. cymatopleura, C. gandrupii* (J.B.Petersen) Lange–Bert. et Krammer, *C. gibsonii* and *C. krasskei* Lange–Bert. the alveoli are not interrupted by a hyaline area (Lange–Bertalot & Metzeltin 1996; Lange–Bertalot & Genkal 1999; Van de Vijver et al. 2012). In *Chamaepinnularia thermophila* (Manguin) C.E.Wetzel et Ector the striae are composed of a row of up to four areolae (Wetzel & Ector 2016).

Until now it was not clear where *Chamaepinnularia* belongs in the "diatom tree of life". The syllabus of plant families placed this genus within the Naviculales, a broad order comprising 18 families including the Pinnulariaceae D.G.Mann (Cox 2015; Round et al. 1990). In Algaebase, the genus is listed as incertae sedis at the family level (Guiry & Guiry 2022).

In addition to diagnostic morphological features, molecular data are valuable in revealing the phylogenetic position of diatom taxa and have been useful in genera where it was difficult to determine their affiliation, e.g. *Gomphonella* Rabenhorst (Jahn et al. 2019), *Spicaticribra* J.R.Johans., Kociolek et Lowe (Downey et al. 2021), the enigmatic genera *Diprora* S.P. Main (Kociolek et al. 2013), and *Karthickia* Kociolek, Glushchenko et Kulikovskiy (Yana et al. 2022). Furthermore, DNA sequences are crucially needed as references for DNA metabarcoding studies to investigate diatom biodiversity in environmental samples. This technique has proved to be a reliable method for studying species diversity and has shown to be a valuable addition to light microscope–based identifications (Kermarrec et al. 2014; Zimmermann et al. 2015; Mora et al. 2019; Pérez–Burillo et al. 2022).

The objectives of this study are to provide the first molecular data of the genus *Chamaepinnularia* based on Arctic and Antarctic strains and to investigate its phylogenetic position based on nucleotide sequence data as well as on detailed morphological examination. Molecular phylogenetics were based on two marker genes, i.e. the nuclear–encoded small subunit rRNA gene (18S) and the plastid gene rbcL. This was complemented with observations of living material from light microscopy (LM), as well as detailed morphological examination of oxidized material on LM and scanning electron microscopy (SEM).

Methods

Study area, field collection and culturing. Freshwater, brackish, and marine samples from epipsammic biofilms were collected at sites from Potter Cove (King George Island, Antarctic Peninsula, Fig. 1) in the austral summer 2020. At two locations cells of the genus *Chamaepinnularia* were found in the environmental samples. One site, located at the shore east of Carlini Station, was characterised by brackish water (D294). The other location was marine, located at Island A4 at 15 m depth (D296 and D297). Unfortunately, no environmental data could be measured during sampling.

Diatom cells were isolated from aliquots of the biofilm samples to establish clonal cultures (Table 1). Using an inverted light microscope (100–400x magnification, Olympus) and microcapillary glass pipettes, single cells were transferred into microwell plates containing culture medium, either Alga–Gro medium (Carolina Biological Supply Company) or Guillards f/2 medium (Guillard & Ryther 1962), 34 psu for marine samples and 12 psu for brackish samples. All water samples, isolates and cultures were maintained at 5–7 °C. Illumination was accomplished by white light LEDs under a 16/8 day/night cycle with 15 min dark phases every hour during the day to prevent photo–oxidative stress.

Furthermore, three other strains were added to this study from samples collected in 2006–2013 (Table 1). The strain CCCryo 272–06 was isolated from a broad snow field at Maxwell Bay, King George Island (Fig. 1). This diatom produced a bloom on the snow field staining parts of the snow in a brownish–green colour (Fig. 2). The other two strains derived from samples from high–Arctic permafrost and snow areas in Svalbard (Fig. 1): one from rocky soil with snow field run–off in Hornsund (CCCryo 390–11) and the other from a snow field on Makarovbreen in Raudfjorden (CCryo 443–14). Electrical conductivity and pH values were measured with a Multi 3420 device with a Tetracon 925 conductivity and a SenTix HW pH probe (WTW, Weilheim, Germany). VISOCOLOR ECO colorimetric test sets by Macherey–Nagel (Düren, Germany) were used for determining ammonium (product no. 931010), total hardness (931029), and carbonate hardness (931014). Cells were isolated under a binocular (GSZ, model 30–G 736, Jenoptik Car Zeiss Jena GmbH) at 10–50× magnification using a sterile glass needle. Single cells were cleaned from adhering bacteria by pulling the algal cell over the surface of an agar

plate containing culture medium. The single cells were then transferred to new, separate agar plates to establish stock cultures. The strains are available as live cultures from the Culture Collection of Cryophilic Algae (CCCryo, Fraunhofer IZI–BB). At CCCryo the isolates are maintained on agar slants with diatom medium either prepared with freshwater (= fwDiatom medium, for CCCryo 390–11 and CCCryo 443–14), or mixed 1:1 with 30 psu artificial seawater (=15 psu swDiatom medium = brackish seawater medium, for CCCryo 272–06). The culture medium recipe is available as Supplementary material 1. Stock cultures are maintained in fridges with glass doors at 2–6 °C with LEDs (Valoya L18, NS12 Spectrum, Valoya Oy, Finland) at a PAR photon flux density of 5–10 $\mu mol.m^{-2}.s^{-1}$ under a 16/8 day/night cycle.

Acquisition of morphometric data and identification

Environmental samples and material harvested from the unialgal cultures were treated with 35% hydrogen peroxide at room temperature to oxidize the organic material and washed with distilled water as described in Mora et al. (2019). To prepare permanent slides for LM analyses, the cleaned material (frustules and valves) was dispersed on cover glasses, dried at room temperature, and embedded with the high refraction index mounting medium Naphrax®.

Observations were conducted with a Zeiss Axioplan Microscope equipped with Differential Interference Contrast (DIC) using a Zeiss 100× PlanApochromat objective using oil immersion. Microphotographs were taken with an AXIOCAM MRc camera. Aliquots of cleaned sample material for SEM observations were dried on silicon wafers and mounted on stubs and observed under a Hitachi FE 8010 scanning electron microscope operated at 1.0 kV.

DNA extraction, amplification, and sequencing. Cultured material was first centrifuged and culture medium was discarded by carefully pipetting. DNA was isolated from the remaining pellet using NucleoSpin® Plant II Mini Kit (Macherey–Nagel, Düren, Germany) following product instructions. DNA fragment size and concentrations were evaluated via gel electrophoresis (1.5% agarose gel) and Nanodrop® (PeqLab Biotechnology LLC; Erlangen, Germany), respectively. Amplification was conducted by polymerase chain reaction (PCR) after Jahn et al. (2017) for 18S. Thereby the 18S rRNA gene locus was amplified in two overlapping parts using two different primer pairs Algen F (CTG GTT GAT CCT GCC AGT AG, start of 18S) and Algen iR (TTC GAT CCC CTA ACT TTC GTT), as well as Algen iF (TTG TCA GAG GTG AAA TTC TTG GA) and D1800R (GCT TGA TCC TTC TGC AGG T) following the PCR regime in Zimmermann et al. (2011). Additionally, the V4 region of 18S was amplified following Zimmermann et al. (2011) as backbone for the alignment using the overlapping parts of the different sequences as counter insurance. The protein–coding plastid gene rbcL was amplified after Abarca et al. (2014) with M13 tailed primers rcbL–iF/rbcL–R. PCR products were visualised in a 1.5% agarose gel and cleaned with MSB Spin PCRapace® (Invitek Molecular GmbH, Berlin,

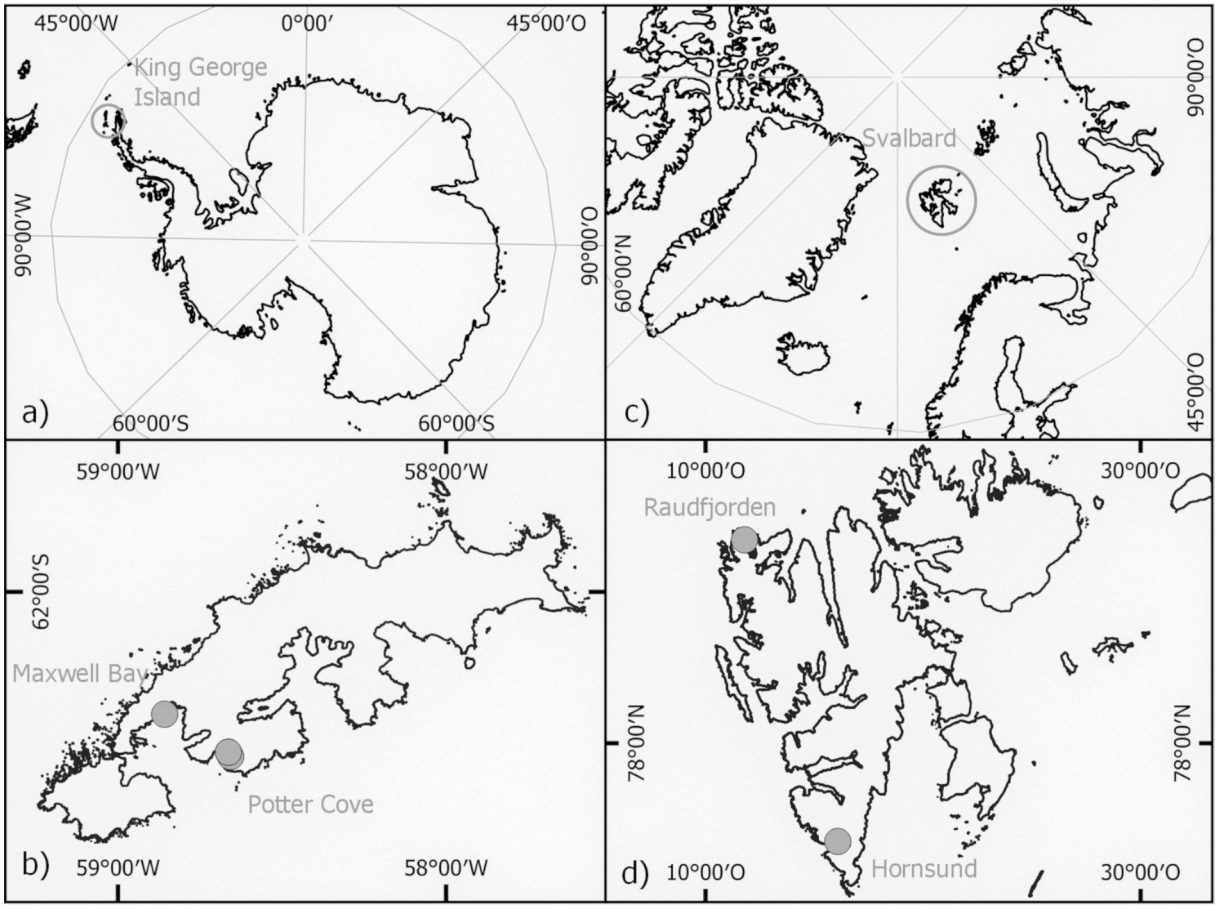

Fig. 1. Sample locations: (a) map of the Antarctic; (b) map of King George Island with sample locations Maxwell Bay and Potter Cove; (c) map of the Arctic; (d) map of Svalbard with sample locations Raudfjorden and Hornsund.

Table 1. Strain name, voucher number, DNA Bank number, taxon name, origin, date, collector as well as Genbank Accession numbers of the studied strains.

Strain	Voucher at BGBM	DNA Bank	Taxon	Origin	Collector	Sampling date	Georeference	Accession number rbcL	Accession number 18S
CCCryo 390–11	B 40 0044447	DB31169	*Chamaepinnularia krookii*	Spitsbergen, Hornsund, freshwater sample, rocky soil with run–off from snow field above	T. Leya	07.08.2010	N77°00‘22.1“ E16°13‘14.1“	OX386458	OX386233
CCCryo 443–14	B 40 0044448	DB31170	*Chamaepinnularia krookii*	Spitsbergen, Raudfjorden, freshwater sample, snow field around melt lake near glacier mouth	T. Leya	06.08.2013	N79°48‘27.6“ E11°50‘27.0“	OX386459	OX386234
CCCryo 272–06	B 40 0044446	DB31168	*Chamaepinnularia australis*	King George Island, Maxwell Bay, freshwater sample, broad green snow field with surface partly melted down to ground ice	T. Leya	09.02.2006	62°10'59.8" S 58°54'52.6" W	OX386457	OX386232
D294_001	B 40 0045203	DB43033	*Chamaepinnularia australis*	King George Island, Potter Cove, brackish water, 0 m deep, epipsammic biofilm	J. Zimmermann	30.01.2020	62°14'07.78" S, 58°39'27.91" W	OX386460	OX386235
D294_002	B 40 0045204	DB43034	*Chamaepinnularia australis*	King George Island, Potter Cove, brackish water, 0 m deep, epipsammic biofilm	J. Zimmermann	30.01.2020	62°14'07.78" S, 58°39'27.91" W	OX386461	OX386236
D294_013	B 40 0045208	DB43043	*Chamaepinnularia australis*	King George Island, Potter Cove, brackish water, 0 m deep, epipsammic biofilm	J. Zimmermann	30.01.2020	62°14'07.78" S, 58°39'27.91" W	OX386464	OX386239
D294_014	B 40 0045209	DB43074	*Chamaepinnularia australis*	King George Island, Potter Cove, brackish water, 0 m deep, epipsammic biofilm	J. Zimmermann	30.01.2020	62°14'07.78" S, 58°39'27.91" W	OX386465	OX386240
D294_005	B 40 0045272	DB43037	*Chamaepinnularia gerlachei*	King George Island, Potter Cove, brackish water, 0 m deep, epipsammic biofilm	J. Zimmermann	30.01.2020	62°14'07.78" S, 58°39'27.91" W	OX386462	OX386237
D294_006	B 40 0045207	DB43038	*Chamaepinnularia gerlachei*	King George Island, Potter Cove, brackish water, 0 m deep, epipsammic biofilm	J. Zimmermann	30.01.2020	62°14'07.78" S, 58°39'27.91" W	OX386463	OX386238
D296_001	B 40 0045355	DB43045	*Chamaepinnularia gerlachei*	King George Island, Potter Cove, marine water, 15 m deep, epipsammic biofilm	J. Zimmermann, G. L. Campana, Divers Carlini Station	31.01.2020	62°13'43.61" S, 58°39'49.36" W	OX258987	OX258985
D296_002	B 40 0045356	DB43046	*Chamaepinnularia gerlachei*	King George Island, Potter Cove, marine water, 15 m deep, epipsammic biofilm	J. Zimmermann, G. L. Campana, Divers Carlini Station	31.01.2020	62°13'43.61" S, 58°39'49.36" W	OX386466	OX386241
D297_003	B 40 0045277	DB43047	*Chamaepinnularia gerlachei*	King George Island, Potter Cove, marine water, 15 m deep, epipsammic biofilm	J. Zimmermann, G. L. Campana, Divers Carlini Station	31.01.2020	62°13'43.61" S, 58°39'49.36" W	OX386467	OX386242

Fig. 2. CCCryo 272–06 produced a brownish–green snow algal bloom on a snow field north of Artigas Base freshwater lake (also known as: Lago Uruguay, Lake Profound or Artigas Base freshwater lake) on Fildes Peninsula in Maxwell Bay (King George Island, South Shetland Islands, Antarctica). © Fraunhofer IZI–BB

Germany) following manufacturer instructions. Concentrations of PCR products were measured using Nanodrop (PeqLab Biotechnology) and normalized to >100 ng.µl^{-1} for sequencing. Sanger sequencing was conducted bidirectionally by Starseq® (GENterprise LLC; Mainz, Germany), with the same primers used for the amplifications.

Sequence data processing, alignment and phylogenetic analyses. Electropherograms obtained by Sanger sequencing were checked manually. The resulting reads from both sequencing directions overlapped and the fragments were assembled in Phyde® (Müller et al. 2010) to obtain final sequences of the amplified markers.

Genetic distances were calculated among the 12 *Chamaepinnularia* strains based on the 18S and rbcL sequence matrices using MEGA 11 (Tamura et al. 2021) and the implemented p–distance option. The alignments were trimmed to achieve same length sequences among the strains with 1530 bp for 18S and 990 bp for rbcL. Furthermore, p–distances among the strains based on shorter barcode markers of those two genes were calculated to investigate if they can distinguish among species in DNA metabarcoding studies. Therefore, the 18S V4 barcode marker proposed by Zimmermann et al. (2011) and Visco et al. (2015) was used (ca. 282 bp without primers). For the rbcL barcode marker proposed by Vasselon et al. (2017) was used (263 bp without primers).

For phylogenetic analysis, our sequence datasets (18S, rbcL) were complemented with sequences from 80 strains obtained from NCBI from within the order of Naviculales (Supplementary material 2). Each dataset was aligned in Muscle (Edgar 2004) as implemented in EMBL–EBI (Goujon et al. 2010) and manually improved in Phyde®. The most variable part of the V4 region of 18S (64 bp) was removed for phylogenetic reconstruction, resulting in a 2,946–position matrix for the 92 strains included in the analyses (18S and rbcL alignments available in Supplementary material 3 and 4).

For the phylogenetic analyses, the model of nucleotide substitution was selected for the dataset using jModelTest 2.1.10 (Darriba et al. 2012) implementing the Akaike Information Criterion (AIC). The general time reversible (GTR) model with a gamma distribution (Γ) and a proportion of invariable sites (I) was chosen. Maximum Likelihood (ML) phylogenetic inference was performed on each individual marker (Supplementary material 5 and 6), as well as for the concatenated dataset using RAxML (Stamatakis et al. 2008; Stamatakis 2014). The nonparametric bootstrap analysis with 1000 replicas was used. Bayesian Inference (BI) of phylogeny was run as implemented in MrBayes 3.2.7 (Ronquist et al. 2012) with the default settings: two runs with four incrementally heated Metropolis–coupled Monte–Carlo Markov Chains with 5 million generations were executed, the runs were sampled every 1000 generations, the first 25% generations being discarded as burn–in and the rest was used to calculate a 50% majority rule consensus tree. Convergence was checked based on marginal density, Effective Sample Size (EES) and by trace plot with the software Tracer (Rambaut et al. 2018). ML and BI analyses were run in the CIPRES Science Gateway (Miller et al. 2010). Phylogenetic trees were visualized in FigTree ver. 1.4.4. (Rambaut 2009) and support values higher than 70% for ML and higher 96% for BI were noted on the branches. An additional ML phylogenetic tree was calculated with the same settings with sequences of additional seven strains (Supplementary material 2). For those strains just one marker or shorter sequences were available. This tree included additional sequences from three strains of the genus *Fallacia* Stickle et D.G. Mann, two from *Rossia* M. Voigt, one from *Eolimna* Lange–Bert. et W.Schiller and one from *Envekadea* Van de Vijver, Gligora, Hinz, Kralj et Cocquyt (Supplementary material 7).

Material and Data curation. Vouchers of all strains were deposited in the algae–collection at Botanischer Garten und Botanisches Museum Berlin (B), Freie Universität Berlin. DNA samples were also stored in the Berlin DNA Bank and are available via the Genome Biodiversity Network (GGBN; Droege et al. 2016; Gemeinholzer et al. 2011). Final DNA sequences were submitted to the European Nucleotide Archive (ENA) (http://www.ebi.ac.uk/ena/) using the software tool annonex2–embl (Gruenstaeudl 2020). Nomenclatural acts (Art. 42 of the International Code of Nomenclature for algae, fungi, and plants, Turland et al. 2018) were registered in Phycobank.

Results

Identification and environmental parameters

Twelve *Chamaepinnularia* strains were examined (Table 2) and identified as three distinct species: *Chamaepinnularia gerlachei* Van de Vijver et Sterken, *Chamaepinnularia krookii* (Grunow) Lange–Bert. et Krammer and *Chamaepinnularia australis* sp. nov.
Five strains (D294_005, D294_006, D296_001, D296_002, D297_003) established from brackish and marine samples taken from shallow water and 15 m depth were identified as *C. gerlachei*. Two strains (CCCryo 390–11 and CCCryo 443–14), established from rocky soil and snow field samples at 38 and 20 m a.s.l. from Arctic Svalbard, were identified as *C. krookii*. At the site, where CCCryo 390–11 was sampled, we measured a pH of 5.3. From the snow field, where CCCryo 443–14 was sampled, several parameters were determined: pH = 5.2, electrical conductivity = 11 µS.cm^{-1}, ammonium= 0.4 mg.l^{-1}, total hardness = 10 mg.l^{-1} CaO, carbonate hardness = below detection limit.

Four strains (D294_001, D294_002, D294_013, D294_014) established from one brackish water sample and one strain (CCCryo 272–06) from a snow field sample at 44 m a.s.l. and presumably also influenced by sea spray from the close–by Antarctic Ocean (no salinity measurements were taken from the fields, yet, the strain is maintained at CCCryo in 15 psu brackish culture medium). All these five strains originated from the Antarctic and are here newly described as *Chamaepinnularia australis*.

Molecular analyses

Pairwise comparisons among the three *Chamaepinnularia* taxa showed low genetic differences in the 18S gene, with the lowest between *C. krookii* and *C. australis* (0.1%, 2 bp; Supplementary material 8), followed by *C. australis* and *C. gerlachei* (0.7–0.8%, 11–12 bp), and the highest between *C. krookii* and *C. gerlachei* (0.8–0.9%, 13–14 bp). Pairwise comparison in the 18S V4 barcode region showed higher differences among the taxa again with the lowest between *C. krookii* and *C. australis* (0.7%, 2 bp; Supplementary material 8), followed by *C. australis* and *C. gerlachei* (2.1%, 6 bp), and the highest between *C. krookii* and *C. gerlachei* (2.8%, 8 bp). The rbcL gene revealed larger differences and separated the species more clearly (*C. australis* and *C. krookii*: 2.9%, 30 bp; *C. australis* and *C. gerlachei* 5.1%, 51 bp; *C. krookii* and *C. gerlachei* 5.3%, 52 bp; Supplementary material 8). Pairwise comparison in the rbcL barcode marker (263 bp) showed higher differences among the taxa (*C. australis* and *C. krookii*: 5.3%, 14 bp; *C. australis* and *C. gerlachei* 7.6%, 20 bp; *C. krookii* and *C. gerlachei* 8.7%, 23 bp; Supplementary material 8). There were no genetic intraspecific variabilities within the taxa *C. krookii* and *C. australis*. Within *C. gerlachei* the 18S gene showed a low variability between strain D297_003 and all the other strains (0.1%). For rbcL, there was no intraspecific variability.

ML analysis as well as BI performed on the two–gene concatenated dataset confirmed that our 12 *Chamaepinnularia* strains form a well–supported, monophyletic group (95% bootstrap support/100% posterior probability, Fig. 3) within the Sellaphoraceae Mereschkowsky. The analyses (Fig. 3) placed *Chamaepinnularia* as sister clade to established members of the Sellaphoraceae (81/96) for which sequence data existed (i.e. *Sellaphora* Mereschkowsky, *Fallacia*, *Rossia* and *Diprora*). The tree which included seven additional, shorter sequences (Supplementary material 7) did not indicate those four genera as one monophyletic group, but placed *Fallacia* as sister clade to *Chamaepinnularia* with *Sellaphora, Rossia* and *Diprora* as sister to the *Chamaepinnularia*/*Fallacia* clade (81). Additionally, both trees placed the Sellaphoraceae including *Chamaepinnularia* as sister clade to the family Pinnulariaceae D.G. Mann (73/96). The single gene trees (Supplementary material 5 and 6) further validated the placement of *Chamaepinnularia* within the Sellaphoraceae, despite the low support values.

In our analyses, the Pinnulariaceae comprised strains of the genera *Pinnularia*, *Caloneis* Cleve, *Envekadea* and *Mayamaea* Lange–Bert. The 18S tree further confirmed *Mayamaea* as member of the Pinnulariaceae (Supplementary material 5). However, the rbcL tree (Supplementary material 6) portrayed a different typology, placing *Mayamaea* as sister clade to *Chamaepinnularia*, embedded within the Sellaphoraceae. Both families belonged to the suborder Sellaphorinae D.G.Mann, which has been placed in the tree in Fig. 3 with a support of 94/100. Any higher ranks such as order could not be determined with the selected strains.

Morphological analysis

Morphological analyses confirm the separation of the strains into three distinct species (Table 3).

***Chamaepinnularia gerlachei* Van de Vijver et Sterken**

Description

Living cells (Fig. 4k–u): A single H–shaped plastid was visible with girdle appressed plates and a bridge slightly next to the center of the valve. No pyrenoid was visible. Just before division of the cell the plastid moved and became appressed to the valve faces (Fig. 4t,u). Before cell division the plastid bridge was visible in girdle view.

LM (Fig. 4a–j and v–ax): The shape of smaller valves was elliptical, becoming linear in larger valves with parallel margins and broadly rounded apices. In some cultures, bulbous valves were visible (Fig. 4at). In girdle view frustules were rectangular. Among cultures, the length of the valves varied between 9.0 and 21.8 µm; the width between 3.1 and 5.9 µm (n= 44). Among valves extracted from the environmental samples, length varied between 17.1 and 20.6 µm, width between 4.1 and 5.4 µm (n=7). The central area was rhomboid, forming a rather straight fascia by parallel striae (16–20 in 10 µm among cultures and 18–20 in 10 µm among valves in the environmental sample). In smaller valves fasciae were narrower.

SEM (Fig. 5a–q): Striae consisted of an alveolus which was covered by a hymen. Due to preparation and oxidation, the hymen was corroded in some valves. In the middle section of the valve, striae were interrupted by a hyaline line (Fig. 5f,g), but they were continuous at the apices. Internally, alveoli were interrupted by a rib–like structure (Fig. 5e,h). Externally, terminal fissures were deflected or hooked to the same side reaching onto the mantle, proximal fissures were drop–like expanded. Internally, proximal raphe fissures were deflected to the same side and terminal raphe fissures terminated in small helictoglossae asymmetrically situated in a round to elliptical terminal area. The central area was elevated internally and, in larger valves, externally as well, where the elevation appeared in a circular shape in between the central raphe fissures.

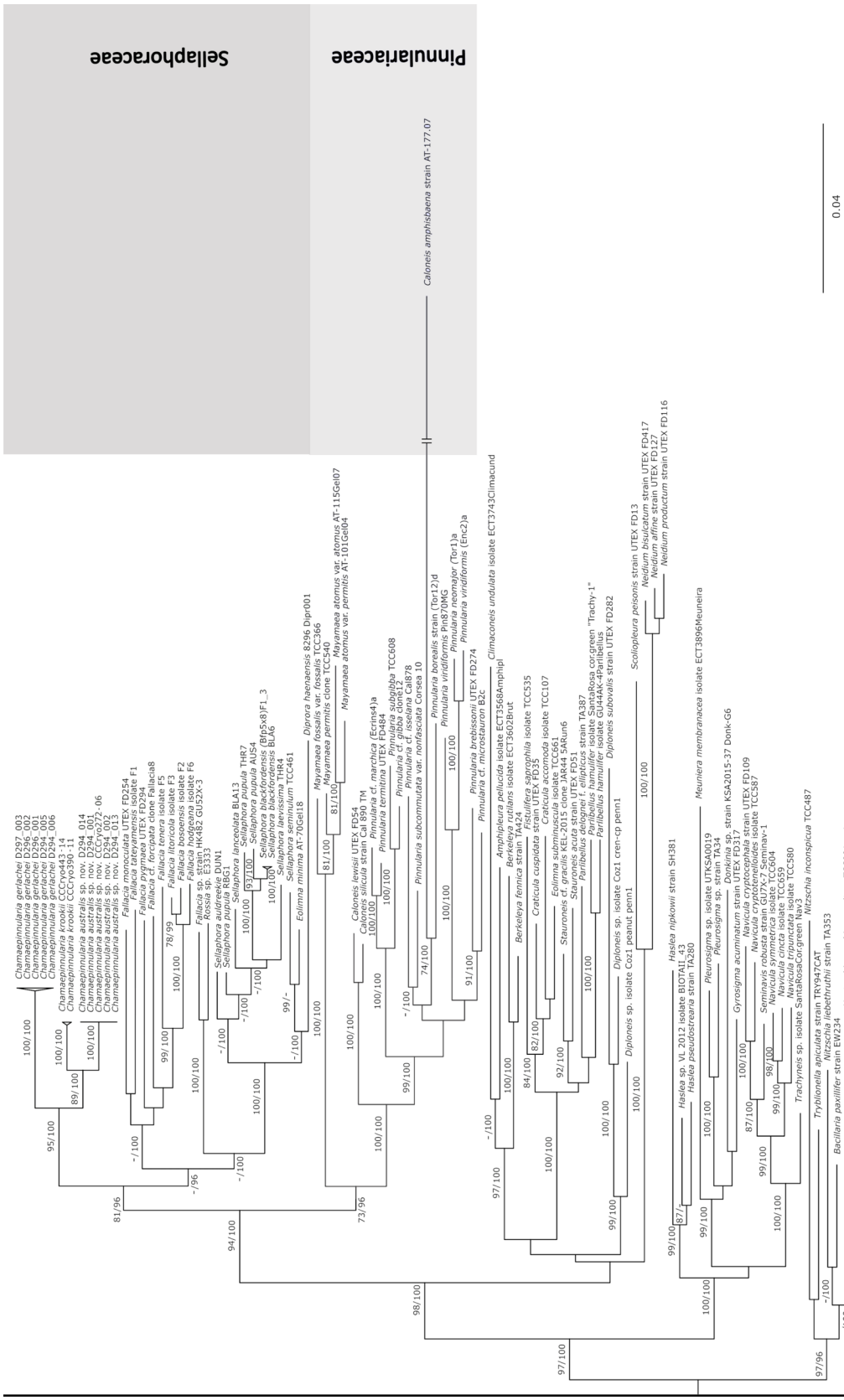

Fig. 3. Maximum likelihood (ML) and Bayesian inference (BI) phylogenetic tree based on the concatenated 18S rRNA and rbcL gene sequences. Nodal support for branches in the ML and BI trees is marked in order (ML/BI). Only bootstrap values over 70% and posterior probability over 96% are shown in the tree.

Table 2. Morphometrics of the studied strains.

Strain	Taxon	n	Length [µm]	Width middle [µm]	Width of apices [µm]	Width of constriction [µm]	Striae in 10 µm	L/W ratio
CCCryo 390–11	*Chamaepinnularia krookii*	11	14.7–15.9	3.7–4.3	3.2–3.5	2.2–3.3	18–20	3.4–4.1
CCCryo 443–14	*Chamaepinnularia krookii*	11	16.9–17.3	3.9–4.5	3.4–3.7	2.4–3.5	18–20	3.8–4.4
CCCryo 272–06	*Chamaepinnularia australis*	17	9.7–17.4	4.2–5.5	2.8–3.5	2.6–3.3	20–24	2.0–3.4
D294_001	*Chamaepinnularia australis*	10	18.4–19.0	4.6–5.0	3.3–3.8	2.6–3.3	18–20	3.7–4.1
D294_002	*Chamaepinnularia australis*	9	18.4–19.0	4.5–5.0	3.3–4.1	2.8–3.4	18–20	3.7–4.2
D294_013	*Chamaepinnularia australis*	11	14.3–15.1	4.5–5.0	3.3–3.8	2.6–3.3	20–21	2.9–3.3
D294_014	*Chamaepinnularia australis*	6	18.2–19.2	4.8–5.2	3.2–3.7	2.6–3.2	18–20	3.6–3.9
D294_005	*Chamaepinnularia gerlachei*	11	9.0–13.2	3.1–4.5			17–20	2.1–3.9
D294_006	*Chamaepinnularia gerlachei*	9	16.2–18.6	3.7–4.0			16–18	4.2–4.8
D296_001	*Chamaepinnularia gerlachei*	17	18.2–20.0	4.2–5.4			18–20	3.5–4.4
D296_002	*Chamaepinnularia gerlachei*	6	18.0–21.2	4.5–5.9			18	3.2–4.1
D297_003	*Chamaepinnularia gerlachei*	9	19.6–21.8	3.9–5.2			16–18	4.1–5.4

Chamaepinnularia krookii (Grunow) Lange–Bert. et Krammer

Description

LM (Fig. 6a–p): The shape of valves was linear biconstricted with convex margins and capitate apices, equal or almost equal in width to the valve middle. In girdle view frustules were rectangular. Among cultures, the length of the valves varied between 14.7 and 17.3 µm; width between 3.7 and 4.5 µm (n= 22). The axial area was very narrow, widening towards the middle forming a rhombic–elliptic to almost round central area. Striae were continuous along the valve, forming no fascia. They were radiate in the middle, becoming parallel, weakly radiate and convergent at the apices (18–20 in 10 µm).

SEM (Fig. 6q–z): Each stria consisted of one alveolus covered by a thick silicate hymen. From the outside of the valves, striae were barely recognizable and showed no discontinuities. In LANGE–BERTALOT & GENKAL (1999), where SEM pictures of two valves were published in external view, a hyaline area dividing the alveoli were also not observable. However, in ZIDAROVA et al. (2016b) the depicted valve was interrupted next to the valve face/mantle junction by a hyaline area. No SEM pictures with an internal view of this species have been published yet. In our strains, alveoli were internally interrupted by a rib–like structure. However, this feature was hardly discernable (Fig. 6y,z) and not visible in every valve. Externally, the proximal raphe fissures expanded spatula–like. Terminal fissures were hooked to one side reaching onto the mantle in contrast to the depicted valve from maritime Antarctica in ZIDAROVA et al. (2016b). Internally, proximal raphe fissures were deflected to the same side and terminal raphe fissures ended in a small helictoglossa asymmetrically situated in a round terminal area. The central area was elevated internally as well as externally, where the elevation appears in a circular shape in between the central raphe pores.

Chamaepinnularia australis Schimani et N.Abarca sp. nov.

Description

Live material (Fig. 7ac–am): A single H–shaped plastid was visible with girdle appressed plates and a bridge lying slightly off–centre within the valve. Pryrenoids were not clearly visible, but one photo (7ae) suggests, that there is one triangular pyrenoid located on both sides of the bridge. Just before division of the cell, the plastid moved and became appressed to the valve face (Fig. 7ad, aj).

LM (Fig. 7a–ab, an–ca): Valves of the type strain (Fig. bc–bg) were elliptic with capitate apices, almost equal in width to the valve middle. Within this culture, the length of the valves varied between 18.4 and 19.0 µm; width between 4.6 and 5.0 µm (*n*=10). The width of the constriction ranged from 3.3 to 3.8 µm. The axial area was very narrow, widening towards the middle forming a rhombic–elliptic central area. Striae radiate in the middle, becoming parallel at the apices (18–20 in 10 µm). A fascia was present in valves of this culture. In extension to the above description of the type strain, valves of the other cultures displayed a high morphological variation especially within the CCCryo 272–06 strain (Fig. 7bm–ca). Valves from oxidized environmental samples exhibited the same morphological variability (Fig. 7a–ab). Shape of the valves was varying between elliptic with broadly rounded to capitate apices.

Among all cultures, the length of the valves varied between 9.7 and 19.2 µm; width between 4.2 and 5.5 µm (n=53). In smaller valves striae were parallel throughout and striae density was higher with 20–24 in 10 µm. The central area was morphologically variable as well forming a small round to larger rhombic–elliptic central area. Fasciae were not present in all valves among cultures and environmental samples. This feature was also observed to be inconsistent within the same

Table 3. Comparison of morphological key characters among the three identified *Chamaepinnularia* species.

	Chamaepinnularia gerlachei	*Chamaepinnularia krookii*	*Chamaepinnularia australis*	*Chamaepinnularia krookiformis* (Krammer 1992; Lange–Bertalot & Genkal 1999)	*Chamaepinnularia plinskii* (Żelazna–Wieczorek & Olszyński 2016)
Plastid	H–shaped plastid with girdle appressed plates	H–shaped plastid with girdle appressed plates	H–shaped plastid with girdle appressed plates	no data	no data
Outline	linear	linear, biconsticted	elliptic	elliptic with strong convex margins	linear
Apices	broadly rounded	capitate, equal in width to the valve middle	broadly rounded to capitate, almost equal in width to the valve middle	capitate, lower in width than the valve middle	capitate, almost equal in width to the valve middle
Cover of areolae	hymen, interrupted by a hyaline line	thick silicate hymen, internally interrupted by a hyaline line	hymen, interrupted by a hyaline line	hymen, interrupted by a hyaline line	hymen, interrupted by a hyaline line
Straition pattern	parallel	radiate in the middle, parallel at apices	radiate in the middle, parallel at apices	radiate in the middle, parallel at apices	radiate in the middle, parallel at apices
Central area	rhomboid	rhombic–elliptic to almost round	small round to larger rhombic–rhomboid	rhomboid	rhomboid
Fascia	straight fascia	no fascia	bow tie shape fascia to no fascia	no facia	bow tie shape fascia

frustule, with a fascia present on one valve but absent on the other valve (Fig. 7h,i).

SEM (Fig. 8a–o, Fig. 9a–n): The striae consisted of one alveolus which was covered by a hymen (Fig. 8i,j). They were externally interrupted by a hyaline line (Fig. 8a,l), internally visible as a rib–like structure except for the striae of the capitate apices (Fig. 8c,m). Externally, the proximal raphe fissures expanded drop–like. Terminal fissures were hooked to one side reaching onto the mantle. Internally, proximal raphe fissures were deflected to the same side and terminal raphe fissures ended in a small helictoglossa asymmetrically situated in a round to small elliptical terminal area. Central area was elevated internally as well as externally, where the elevation appeared in a circular to elliptic shape in between the central pores. In CCCryo 272–06 some valves did not fit the above description. In some smaller valves, striae appeared very broad almost reaching the raphe (Fig. 9l) and in some large valves, striae were parallel and not interrupted by a hyaline area (Fig. 9m).

Holotype*:* slide B 40 0045203a, Botanic Garden and Botanical Museum, Berlin, Fig. 7bd from the strain D294_001 illustrates the holotype. SEM–stub deposited as B 40 0045203b. For molecular material and data see Methods.

Type Locality: Potter Cove, King George Island, South Shetland Islands, collected by J. Zimmermann on 30.01.2020, coordinates: S 62.235314, W 58.656489.

Registration*:* http://phycobank.org/103413.

For INSDC Accession numbers see Table 1.

Habitat*:* brackish water, shallow coastal zone (epipsammic biofilm) and freshwater (snow field).

Etymology: The species name refers to its geographic distribution on the southern hemisphere, the Antarctic region in particular.

Differential diagnosis: *Chamaepinnularia australis* can be differentiated by genetic distances from *C. krookii* and *C. gerlachei*, especially in 18S V4 barcode (0.7–2.8%) and rbcL marker (2.9–5.3%).

Based on morphology (Table 3), *C. gerlachei* can be separated from *C. australis* by the outline as it has parallel margins with broadly rounded apices, and by the parallel striae. *C. krookii* has a linear biconstricted outline and no fascia.

Our strains of *C. australis* differ in several characters from *C. krookiformis* (Krammer) Lange–Bert. et Krammer as described in Krammer (1992): The valve outline in *C. krookiformis* is more elliptical with strong convex margins and round apices, which were considerably narrower than the valve width. *C. krookiformis* has no fascia.

C. plinskii Żelazna–Wieczorek et Olszyński shares similarities with some of our cultures (D294_001, D294_002, D294_014). However, valves of *C. plinskii* have more linear valve margins. Furthermore, *C. plinskii* has a slightly higher number of striae in 10 μm

Table 4. Comparison of key characters of *Chamaepinnularia* with some genera from the Sellaphorinae.

	Chamaepinnularia	***Sellaphora/Eolimna***	***Fallacia/Pseudofallacia***	***Rossia***	***Diprora***	***Pinnularia/Caloneis***	***Envekadea***	***Mayamaea***
References	LANGE–BERTALOT & METZELTIN 1996 ZIDAROVA et al. 2016b CANTONATI & LANGE–BERTALOT 2009 WETZEL et al. 2013 this study	MERESCHKOWSKY 1902 ROUND et al., 1990 MANN 1989 WETZEL et al. 2015	ROUND et al. 1990 LIU et al. 2012 LI et al. 2022	LI et al. 2022	MAIN 2003 KOCIOLEK et al. 2013	ROUND et al. 1990 SOUFFREAU et al. 2011 KRAMMER 2000 ZIDAROVA et al. 2016b	GLIGORA et al. 2009 MALTSEV et al. 2017	LANGE–BERTALOT 1997 ZIDAROVA et al. 2016b KEZLYA et al. 2020
Cell organisation	solitary	solitary	solitary	solitary	straight colonies	solitary	solitary	solitary
Plastid	H–shaped, consisting of two girdle–appressed plates connected by an isthmus	H–shaped, consisting of two girdle–appressed plates connected by an isthmus	H–shaped, consisting of two girdle–appressed plates connected by an isthmus	no data	H–shaped, consisting of two girdle–appressed plates connected by an isthmus	H–shaped or two girdle appressed plastids	H–shaped, consisting of two girdle–appressed plates connected by an isthmus	two chromatophores (LANGE–BERTALOT 1997) *M. vietnamica*: H–shaped, consisting of two girdle–appressed plates connected by an isthmus (KEZLA et al. 2020)
Outline	linear to elliptical, bluntly rounded to capitate apices	linear to elliptical, bluntly rounded to capitate apices	linear to elliptical with broadly rounded apices	linear to elliptical	linear to elliptical with rounded apices	linear, lanceolate or elliptic with broadly rounded to capitate apices	linear–lanceolate with (sub)– capitate apices	linear to elliptical with rounded apices
Striae	uniseriate	uniseriate (to biseriate)	uniseriate	uniseriate	uniseriate	multiserate	uniseriate	uniseriate (to biseriate)
Areolae	elongated, one large areola divided by one or more hyaline areas	small, rounded poroids	small round, in *Pseudofallacia*: elongated	small round	single row of round to ovoid areolae down each side near margin	chambered alveolus	large, rectangular to polygonal pores, can be irregular in shape	round, elliptical, square shape, near the mantle occasionally slit–like
Conopeum	absent	nonporous conopeum or absent	finely porous conopeum	restricted to the raphe sternum with irregular arrangement of pores	absent	absent	absent	absent

Table 4. Cont.

Special features at axial area	no special features *C. schauppiana* peculiar grooves on the axial area (Cantonati 2009)	some species: The raphe sternum is flanked by longitudinal irregular grooves	lyre–shaped, parallel or lanceolate canals, *Pseudofallacia*: two longitudinal depressions along the narrow sternum	wide longitudinal canals	araphid with a broad sternum	no special features	no special features	pronounced sternum
External covering of areolae	occluded by hymenes	absent	*F. tenera* group occluded areolae near valve margin *Pseudofallacia:* occluded by hymen	no data	occluded by hymenes sunken into the areolae with a network of round openings in a single plane	occluded by porous hymenes	occluded by hymenes, perforated by an irregular number of very small rounded pores	occluded by hymenes
Internal covering of areolae	absent	occluded by hymenes	occluded by hymenes (Liu et al. 2012)	no data	absent	internal covering of alveoli by axial or laminar plates	absent	absent
External central raphe ending	drop–like, spatulate, not deflected to slightly deflected	expanded, slightly deflected	straight, expanded or weakly dilated	no data	–	round to droplike, dilated	expanded, forming conical depressions, straight	spatulate to drop shape expanded, straight to deflected
External terminal raphe ending	deflected or hooked to the same side	deflected or hooked to the same side	deflected, bent or hooked to the same side	no data	–	hooked to the same side, often opposite to central raphe ending	bent to opposite sides, giving the raphe a sigmoid from	bent to the same side, opposite to central raphe endings
Internal central raphe ending	deflected or hooked to one side	deflected to one side	deflected to one side	no data	–	hooked to one side, Intermissio in some genera present	straight or very slightly deflected to one side	deflected to one side
Internal terminal raphe ending	helictoglossa small, asymmetrical situated in round to elliptical terminal area	helictoglossa small, in large–celled species often large and elongated	helictoglossa small	no data	–	helictoglossae variable	helictoglossae small situated in a wedge–shaped terminal area	helictoglossa small
Girdle bands	non perforated	non perforated	non perforated	no data	fimbriate margin, non perforated	one row of elongated poroids on the first band	non perforated	non perforated

(20–26/10 µm vs. 18–21(24)/10 µm). In contrast to *C. plinksii,* the presence of a fascia is inconsistent in *C. australis*, even within one frustule (Fig. 7h,i and 7j,k). In addition, among our cultures, valves have a wider range in dimension (9–22 vs. 18–24 µm). The outline in *C. australis* is highly variable, from broadly rounded to capitate apices. The central area ranges from a small round to a wide rhomboid shape in contrast to an always wide rhomboid central area in *C. plinksii*. Thus, the morphological variation in *C. australis* hugely exceeds the description of *C. plinskii* and the separation of those two taxa is needed.

Discussion

Monophyly of the genus *Chamaepinnularia*

The nucleotide sequence data from strains of *Chamaepinnularia* presented in this study support the recognition of *Chamaepinnularia* as a distinct genus from *Navicula* or *Pinnularia* as already proposed by Lange–Bertalot & Metzeltin (1996), or from any other genera within the Naviculales included in the molecular phylogenies of this study. Genetic distances and morphological differences within the 12 analysed strains led to the separation of three distinct taxa. All three species can be separated through both barcode markers for 18S V4 and rbcL and are thereby unambiguously distinguishable in DNA Metabarcoding studies.

Chamaepinnularia krookii seems to be a cosmopolitan species found from the Arctic to Antarctica (Krammer 1992; Lange–Bertalot & Genkal 1999; Zidarova et al. 2016b) and from such extreme habitats as snow fields on glaciers (CCCryo434–14). This species was first published as *Navicula krookii* by Grunow (1882) from fossil material of brackish environments in Sweden and the Czech Republic. The species underwent several transfers and new combinations (see Żelazna–Wieczorek & Olszyński 2016) until it was finally transferred to *Chamaepinnularia* by Lange–Bert. et Krammer in Lange–Bertalot & Genkal (1999). *Chamaepinnularia gerlachei* was first published in Van de Vijver et al. (2010) from dry soil samples on James Ross Island, north of the Antarctic Peninsula, and has been observed until now only in maritime Antarctica and is probably endemic (Kopalová et al. 2012; Sterken et al. 2015; Zidarova et al. 2016b). Our sample location at 15 m water depth from a sediment biofilm in a marine environment is quite different from the type locality. Prelle et al. (2022) verified a broad salinity tolerance for this species, supporting its presence and adaptation to different habitats. Growth of this species in culture was proven at 0–65 S_A (absolute salinity) and a photosynthetic potential up to 100 S_A. Similarly, a broad spectrum of habitats is occupied by *Chamaepinnularia australis*, sampled from a snow field to immersed brackish environments. This suggests a high tolerance to salinity, radiation, and aridity.

This newly described species had been found in several studies of freshwater samples in maritime Antarctica and identified so far as *C. krookiformis* (Kopalová et al. 2012; Sterken et al. 2015; Zidarova et al. 2016b; Silva et al. 2019). *Chamaepinnularia krookiformis* was first published as *Pinnularia krookiformis* by Krammer (1992) from a periodic saline pool in North Rhine–Westphalia (Germany) and was then transferred to *Chamaepinnularia* by Lange–Bert. et Krammer in Lange–Bertalot & Genkal (1999). However, all depicted valves from the Antarctic differ from the type material of *C. krookiformis* by the outline and the presence of a fascia and hence the new species is described. *C. australis* from Antarctic waters showed only in a few valves a similar morphology as in valves described as *C. plinskii* (Żelazna–Wieczorek & Olszyński 2016). The authors revised *C. krookiformis*, identifying three morphodemes, and describing one as a new species, *C. plinskii* from brackish inland waters in Poland. However, the new species described here exhibits a morphological variability far exceeding that of *C. plinskii*. Already Zidarova et al. (2016b) stated that in Antarctic populations the presence of a fascia is not a constant feature, which is a constant feature of *C. plinskii*.

As shown here with *C. plinskii* sensu Żelazna–Wieczorek et Olszyński (2016) and the description of *C. australis*, studies have shown that some species with morphological similarities may actually constitute two or more different species with distinct biogeographical patterns which can only be revealed with the use of sequence data, e.g., *Gomphonema parvulum* (Kützing) Kützing (Kermarrec et al. 2013; Abarca et al. 2014), *Pinnularia borealis* Ehrenberg (Pinseel et al. 2020), *Planothidium lanceolatum* (Bréb. ex Kütz.) Lange–Bert. and *P. frequentissimum* (Lange–Bert.) Lange–Bert. (Jahn et al. 2017).

Valves identified as *C. krookiformis* from the Arctic exhibit a certain variability as well and were depicted with a more linear outline and a fascia (Lange–Bertalot & Genkal 1999). Further investigations of *Chamaepinnularia* in the northern hemisphere, ideally a combination of morphological and molecular data, will uncover to which species those valves belong.

A large morphological variability was apparent within *C. australis*. Morphological variability often increases with the cultivation time. Especially the shape is altered and cell lengths are reduced (Mohamad et al. 2022). This was especially obvious in the strain CCCryo 272–06 which has been a long–term culture since 2006, being 16 years old (without any interim sexual reproduction observed). Yet, valves of this species observed from environmental samples also demonstrated a high variation in valve shapes and sizes as well. Worth mentioning is its obviously well adaptation to such an extreme habitat as a snow field, on which it developed a macroscopically visible bloom. Though not measured in this case but known from other snow fields (compare Fig. 4 in Spijkerman et al. 2012) are low contents in nitrate,

ammonium and phosphate still enabling this species to form algal blooms. Possibly there is a relatively high turnover of nutrients due to other contributing snow field organisms (bacteria, fungi a.o.) supporting such algal blooms. Furthermore, diatom morphology shifts in response to various environmental factors like temperature, salinity, nutrient concentration, and UV radiation (reviewed in Su et al. 2018 and Fu et al. 2022), which may add to the morphological variation of the frustule in this species as well.

Comparison of morphological characters of closely related genera

According to Kulikovskiy et al. (2018), the family Sellaphoraceae comprises the genera *Sellaphora*, *Fallacia*, *Rossia*, *Caponea* Podz., *Okhapkinia* Glushchenko, Kulikovskiy et Kociolek, *Buryatia* Kulikovskiy, Lange–Bert. et Metzeltin, *Pseudofallacia* Y.Liu, Kociolek et Q.X.Wang, *Lacuneolimna* Tudesque, Le Cohu et Lange–Bert., *Eolimna* Lange–Bert. et W.Schiller and *Diprora*. Our results confirmed monophyly of this family based on the genera for which sequence data have been generated (i.e. *Sellaphora*, *Fallacia*, *Rossia*, *Diprora*, and now *Chamaepinnularia*), supporting previous studies (Nakov et al. 2018; Li et al. 2022). Pinnulariaceae was recovered as a sister clade to Sellaphoraceae as already stated in previous studies (Nakov et al. 2018; Li et al. 2022). This family comprises the genera *Pinnularia, Envekadea, Diatomella* Greville*, Hygropetra* Krammer et Lange–Bert.*, Oestrupia* Heiden ex Hustedt, *Craspedopleura* Poulin and *Caloneis* (Round et al. 1990; Poulin 1993; Krammer 2000; Maltsev et al. 2017).

The comparison of morphological characters of *Chamaepinnularia* with genera whose placement in Sellaphoraceae or Pinnulariaceae was supported with molecular data, is shown in Table 4. This includes the genera *Sellaphora*/*Eolimna*, *Diprora*, *Fallacia*/*Pseudofallacia*, *Rossia*, *Pinnularia*/*Caloneis* and *Envekadea*. Our molecular results recover *Eolimna minima* within the *Sellaphora* clade as already shown by Nakov et al. (2018) suggesting that those strains belong to *Sellaphora*. A study by Wetzel et al. (2015) could not find morphological characters that separate *Eolimna* from *Sellaphora* and almost all species of this genus were transferred to the genus *Sellaphora*. Furthermore, *Diprora* was recovered within the *Sellaphora* group, suggesting that the latter was also not a monophyletic genus. The phylogenetic position of *Pseudofallacia* is uncertain as well and most probably this genus should be merged with *Fallacia* (Li et al. 2022). Little information is known of the genus *Rossia* (Sabbe et al. 1999). The strain *Fallacia* sp. HK482 has been proposed to belong to *Rossia* by Li et al. (2022) and is also recovered within this genus in our phylogenetic analyses. The morphology of *Caloneis* is similar to that of *Pinnularia*, which led Round et al. (1990) to include *Caloneis* within *Pinnularia*. Molecular data also suggested that neither *Pinnularia* nor *Caloneis* are monophyletic (Souffreau et al. 2011; Narkov al. 2018). In Maltsev et al. (2017), *Envekadea* was placed within the *Pinnularia* and *Caloneis* clade suggesting that the large genus *Pinnularia* was not monophyletic and could be split into a few morphologically different taxa.

All genera within Sellaphoraceae and Pinnulariaceae share a similar outline, usually linear, lanceolate to elliptical with broadly rounded to capitate apices. Like *Chamaepinnularia*, every genus in Sellaphoraceae has H–shaped plastids consisting of two girdle–appressed plates connected by an isthmus (Mann 1989; Liu et al. 2012; Kociolek et al. 2013; Li et al. 2022). For the genus *Rossia* no data are available. Within Pinnulariaceae the genus *Envekadea* and some species of *Pinnularia* possess H–shaped plastids or more often two girdle appressed plastids, which are only connecting just before cell division (Cox 1996; Souffreau et al. 2011).

Chamaepinnularia has uniseriate striae like *Envekadea* and most members of the family Sellaphoraceae (Gligora et al. 2009; Liu et al. 2012; Wetzel et al. 2015; Li et al. 2022). In contrast to *Sellaphora*'s small and round areolae (Wetzel et al. 2015), *Chamaepinnularia* possesses alveoli similar to *Pseudofallacia* (Liu et al. 2012) or *Pinnularia*, which has alveoli, where the outer surface is ornamented by multiple rows of small pores forming multiseriate striae (Round et al. 1990; Souffreau et al. 2011).

Genera within Sellaphoraceae often show a complex axial area. The different *Fallacia* clades in Li et al. (2022) are characterised by canals, which can be lyre–shaped, parallel or lanceolate, while *Rossia* possesses wide porous canals (Li et al. 2022). *Pseudofallacia* has two longitudinal ribs along the narrow sternum (Liu et al. 2012). The valve face of *Sellaphora* is flat, except that it is often grooved near the raphe externally (Wetzel et al. 2015). This feature is however missing in *Chamaepinnularia*. Furthermore, a conopeum, which evolved from not being noticeable or with a narrow extension in *Sellaphora* to covering the entire valve face at *Fallacia* (Li et al. 2022), is absent in *Chamaepinnularia*. The genus *Diprora* is exceptional within the Sellaphoraceae, as it is araphid with a broad sternum and a single row of relatively wide round to ovoid areolae down each side near the margin (Main 2003). As suggested by Kociolek et al. (2013), its cave dwelling habit may have led to the loss of its raphe system.

External covering of areolae or alveoli by unstructured or finely porous hymen like in *Chamaepinnularia* can be found in *Pseudofallacia* and some *Fallacia* species (Li et al. 2022). In *Pinnularia* and *Envekadea* they are occluded by porous hymenes (Krammer 2000; Gligora et al. 2009). Internal covering of areolae by unstructured hymenes was found in *Sellaphora* (Wetzel et al. 2015). The hymen of *Diprora,* which possesses a network of round openings, is sunken into the areolae (Kociolek et al. 2013).

Comparable to *Chamaepinnularia* the external central raphe endings in genera of both families are often expanded and sometimes dilated. External terminal raphe

endings are bent or hooked to the same direction (Round et al. 1990; Liu et al. 2012; Wetzel et al. 2015; Li et al. 2022). An exception is *Envekadea*, where the terminal raphe endings are bent into different directions, giving the raphe a sigmoid shape (Gligora et al. 2009). Internal central raphe endings in all genera are deflected to the same side as in *Chamaepinnularia.* However, in some *Pinnularia* species the raphe is continuous or forming an intermissio (Krammer 2000). Internally the raphe of *Chamaepinnularia* and all genera of Sellaphoraceae and Pinnulariaceae end in a helictoglossa (Krammer 2000; Gligora et al. 2009; Liu et al. 2012; Wetzel et al. 2015; Li et al. 2022). The three *Chamaepinnularia* species possess a small helictoglossa situated asymmetrically in a round to elliptical terminal area, a character found in some *Pinnularia* species as well (e.g. *P. australomicrostauron* Zidarova, Kopalová et Van de Vijver*, P. microstauroides* Zidarova, Kopalová et Van de Vijver*, P. pinseeliana* Zidarova, Kopalová et Van de Vijver; Zidarova et al. 2016b).

Girdle bands are non–porous in all genera in Sellaphoraceae and *Envekadea* (Gligora et al. 2009; Liu et al. 2012; Wetzel et al. 2015; Li et al. 2022) as well as in *Chamaepinnularia*. The first band of *Pinnularia* bears one row of elongated poroids (Round et al. 1990).

The newly described genus *Fontina* Beauger, C.E.Wetzel et Ector (Beauger et al. 2022b) shares a number of features with *Chamaepinnularia,* like uniseriate striae interrupted near the valve face/mantle junction, externally closed areolae by hymenes, an absent conopeum and unperforated girdle bands. Unlike *Chamaepinnularia* this genus has asymmetric valves and the internal proximal and the external distal raphe endings are only slightly deflected to the same side in the new genus. *Fontina* was published without molecular data and a cladistic test was not possible (Beauger et al. 2022b).

Phylogenetic placement based on valve morphology alone could turn out to be misleading. This is true especially for taxa within Sellaphorinae. Mann (1989) resurrected the separation of *Sellaphora* from *Navicula* based not only on frustule structure but also on differences in the protoplast, sexual reproduction and changes during the cell cycle. Already Mereschkowsky (1902) distinguished *Sellaphora* by a unique chromatophore–plate being always composed of two parts – a narrow median part resting on the surface of one of the valves, and four long, usually narrow, linear prolongations. In addition to studying living cells, molecular phylogenies are a useful tool for revealing the position and relationships of diatom genera or higher groups (Bruder et al. 2008; Souffreau et al. 2011; Abarca et al. 2020; Downey et al. 2021). As described above, the genus *Envekadea* exhibits some similarities with Sellaphoraceae and lacks characteristics of *Pinnularia* and *Caloneis*, like alveolate striae. Nevertheless, molecular phylogenetics revealed that *Envekadea* belongs to the Pinnulariaceae (Maltsev et al. 2017). Another example is the previously mentioned araphid genus *Diprora* (Kociolek et al. 2013).

Phylogenetic placement of *Chamaepinnularia*

Phylogenetic analyses retrieved *Chamaepinnularia* either as a sister group to Sellaphoraceae (rbcL tree, 18S tree and concatenated tree Fig. 3) or embedded within the Sellaphoraceae (concatenated tree in Supplementary material 7). However, bootstrap support values for the crown nodes of the Pinnulariaceae and of the Sellaphoraceae (73/96 and 81/96 in concatenated trees respectively) are at the edge of confidence and low statistical support within the family in our analyses did not allow us to conclude which genus is most closely related to *Chamaepinnularia*. Morphological examinations showed the presence of unstructured hymen and the possession of a single H–shaped plastid with girdle appressed plates, which are diagnostic characters of the family Sellaphoraceae. We therefore propose the inclusion of *Chamaepinnularia* within the Sellaphoraceae.

The genus *Mayamaea* also possesses morphological characters shared by both families (Sellaphoraceae and Pinnulariaceae). It has uniseriate (to biseriate) striae, external areolae covered by hymenes and a small helictoglossa (Lange–Bertalot 1997; Zidarova et al. 2016b; Kezlya et al. 2020). In live material of *M. vietnamica* Kezlya et al. (2020) observed one H–shaped plastid, with one arm lying against each side of the girdle, connected by a narrow central isthmus. In contrast, Lange–Bertalot (1997) mentioned two chromatophores in each cell with one pyrenoid, when he described the genus. Our concatenated analysis concurs with the findings of Li et al. (2022) and Nakov et al. (2018), placing *Mayamaea* in the Pinnulariaceae.

Our results highlight the importance of an integrative approach that considers findings from cultures with morphological and molecular data to classify taxa with respect to both their species membership and their phylogenetic–systematic placement within higher order classification. Thus, it will be possible to better understand the biodiversity and biogeography of diatoms in general and of diatoms of the polar regions in particular.

Author Contributions

DM, KS, RJ developed the idea and elaborated the concept. JZ and TL sampled, OS and TL provided the isolates. KS and NA provided taxonomical data. KS, DM and JZ performed molecular analysis. WHK, RJ, NA and KS performed the nomenclature act. KS and DM wrote the manuscript and TL provided part of the text. The manuscript was commented, edited, and finally accepted by all authors.

Acknowledgements

We would like to thank the team of the Argentinian Antarctic Research Station "Carlini" of the Instituto Antártico Argentino (IAA) for their support and logistics, especially Gabriela L. Campana and María Liliana Quartino. The authors are grateful to Jana Bansemer for work in the molecular lab and to Juliane Bettig for support at the SEM at the BGBM Berlin.

Funding

This project was funded within the framework of the SPP 1158 Antarktisforschung by the DFG under the grant number ZI 1628/2–1. Collection of the Antarctic strains by TL were funded under the same SPP under grant number Le1275/2–2.

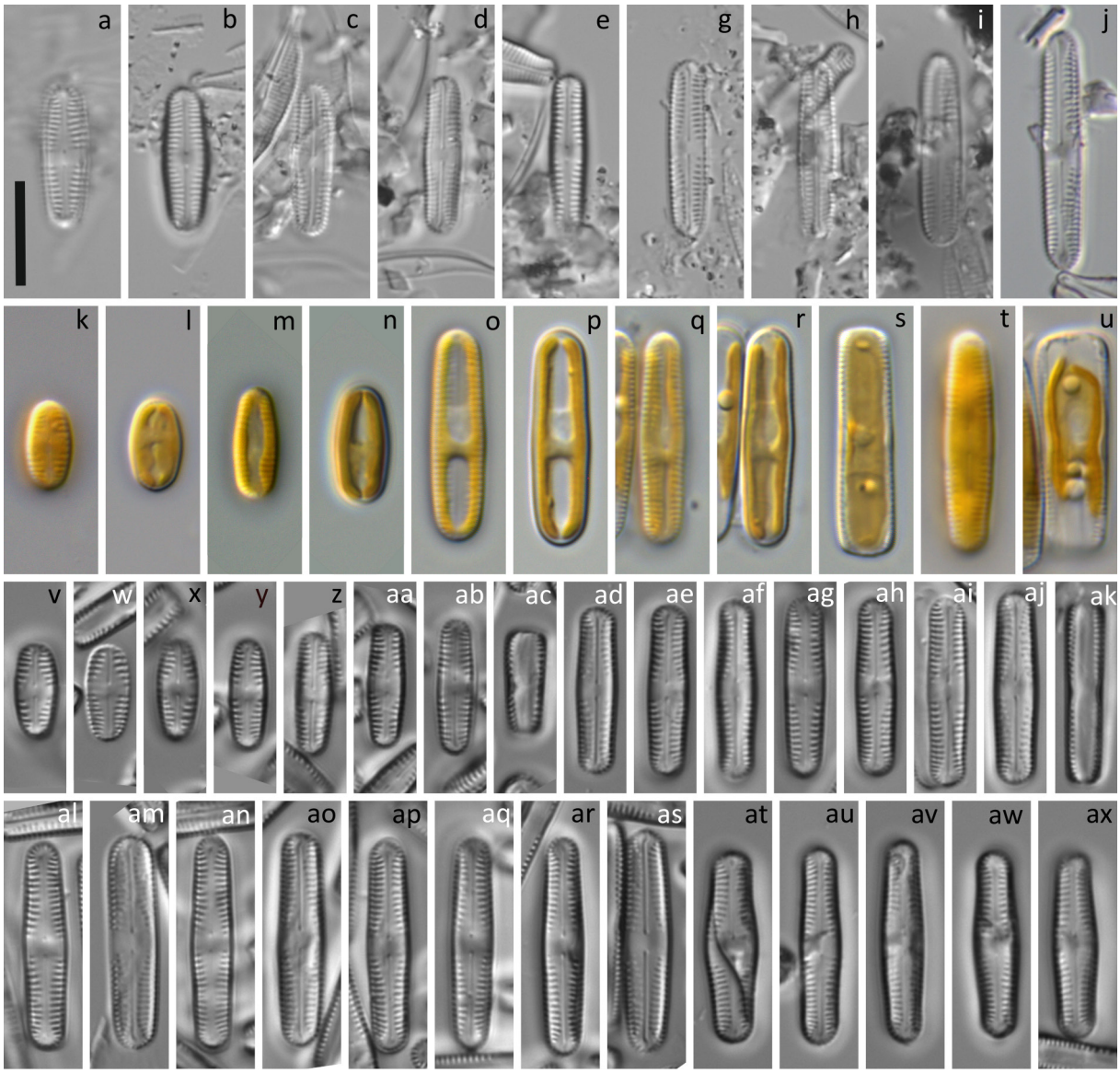

Fig. 4. *Chamaepinnularia gerlachei* LM: (a–j) valves from environmental samples; (k–ax) valves from cultures; (k–u) living cells with H–shaped plastid; (k–n, v–ac) strain D294_005; (o–s, al–as) strain D297_003; (t–u, at–av) strain D296_001; (ad–ak) strain D294_006; (aw–ax) strain D296_002. Scale bar 10 µm.

References

Abarca, N.; Jahn, R.; Zimmermann, J. & Enke, N. (2014): Does the cosmopolitan diatom *Gomphonema parvulum* (Kützing) Kützing have a biogeography? – PloS ONE 9: e86885.

Abarca, N.; Zimmermann, J.; Kusber, W.–H.; Mora, D.; Van, A.T.; Skibbe, O. & Jahn, R. (2020): Defining the core group of the genus *Gomphonema* Ehrenberg with molecular and morphological methods. – Botany Letters 167: 114–159.

Beauger, A.; Wetzel, C. E.; Allain, E.; Bertin, C.; Voldoire, O.; Breton, V.; Baker, L.–A.; Kolovi, S.; David, B. & Ector, L. (2022a): *Chamaepinnularia salina* (Bacillariophyta), a new diatom species from French mineral springs (Massif Central). – Phytotaxa 538: 55–73.

Beauger, A.; Wetzel, C. E.; Voldoire, O.; Allain, E.; Breton, V.; Miallier, D. & Ector, L. (2022b): *Fontina* gen. nov. (Bacillariophyta): a new diatom genus from a thermo–mineral spring of the French Massif Central (France). – Diatom Research 37: 51–61.

Bruder, K.; Sato, S. & Medlin, L. (2008): Morphological and molecular investigations of naviculoid diatoms IV. *Pinnularia* vs. *Caloneis*. – Diatom 24: 8–24.

Cantonati, M. & Lange–Bertalot, H. (2009): On the ultrastructure of *Chamaepinnuaria schauppiana* Lange–Bertalot & Metzeltin (Naviculaceae s. l.). – Diatom Research 24: 225–231.

Cavacini, P.; Tagliaventi, N. & Fumanti, B. (2006): Morphology, ecology and distribution of an endemic Antarctic lacustrine diatom: *Chamaepinnularia cymatopleura* comb. nov. – Diatom Research 21: 57–70.

Cox, E. J. (1996): Identification of freshwater diatoms from live material. – 158 pp., Chapman & Hall, London.

Cox, E. J. (2015): Coscinodiscophyceae, Mediophyceae, Fragilariophyceae, Bacillariophyceae (Diatoms). – In: Jaklitsch, W.; Baral, H.O.; Lücking, R.; Lumbsch, H.T. & Frey, W. (eds): Syllabus of Plant Families. Adolf Engler's Syllabus der Pflanzenfamilien. Part 2/1. Photoautotrophic eukaryotic algae: Glaucocystophyta, Cryptophyta, Dinophyta/Dinozoa, Haptophyta, Heterokontophyta/Ochrophyta, Chlorarachniophyta/Cercozoa, Euglenophyta/Euglenozoa, Chlorophyta, Streptophyta. – pp. 64–103, Borntraeger Verlagsbuchhandlung, Stuttgart.

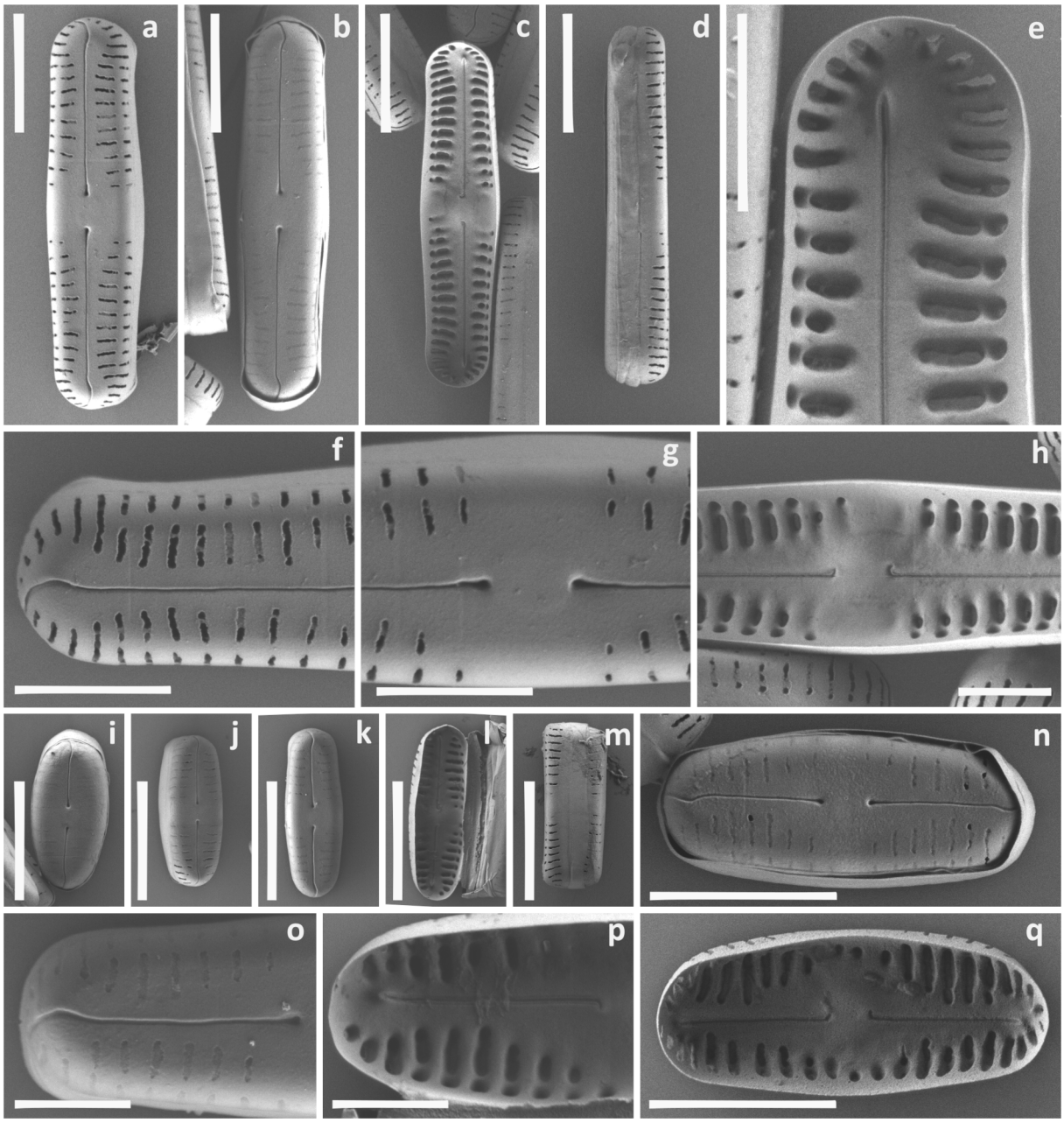

Fig. 5. *Chamaepinnularia gerlachei* SEM: (a–h) strain D294_006; (i–q) strain D294_005; (a–(b, f–g, i–k, n, o) external view; (c, e, h, l, p, q) internal view; (d, m) girdle view; (e) internal striae with silicate bridge and proximal raphe ending; (f, n–o) external striae separated by a hyaline line; (g) external central area; (h) internal central area; (o) external striae occluded by a hymen. Scale bars (a–d, i–n, q) 5 µm, (f–h) 3 µm, (e, o–p) 2 µm.

Darriba, D.; Taboada, G.; Doallo, R. & Posada, D, (2012): jModelTest 2: more models, new heuristics and parallel computing. – Nature Methods 9: 772.

Droege, G.; Barker, K.; Seberg, O.; Coddington, J.; Benson, E.; Berendsohn, W. G.; Bunk, B.; Butler, C.; Cawsey, E. M.; Deck, J.; Döring, M.; Flemons, P.; Gemeinholzer, B.; Güntsch, A.; Hollowell, T.; Kelbert, P.; Kostadinov, I.; Kottmann, R.; Lawlor, R. T.; Lyal, C.; Mackenzie–Dodds, J.; Meyer, C.; Mulcahy, D.; Nussbeck, S. Y.; O'Tuama, É.; Orrell, T.; Petersen, G.; Robertson, T.; Söhngen, C.; Whitacre, J.; Wieczorek, J.; Yilmaz, P.; Zetzsche, H.; Zhang, Y. & Zhou, X. (2016): The Global Genome Biodiversity Network (GGBN) Data Standard specification. – Database 2016: baw125.

Downey, K. M.; Julius, M. L.; Theriot, E. C. & Alverson, A. J. (2021): Phylogenetic analysis places *Spicaticribra* within *Cyclotella*. – Diatom Research 36: 93–99.

Edgar, R. C. (2004): MUSCLE: multiple sequence alignment with high accuracy and high throughput. – Nucleic Acids Research 32: 1792–1797.

Fu, W.; Shu, Y.; Yi, Z.; Su, Y.; Pan, Y.; Zhang, F. & Brynjolfsson, S. (2022): Diatom morphology and adaptation: Current progress and potentials for sustainable development – Sustainable Horizons 2: 100015.

Gemeinholzer, B.; Droege, G.; Zetzsche, H.; Haszprunar, G.; Klenk, H.–P.; Güntsch, A.; Berendsohn, W. & Wägele, J. W. (2011): The DNA Bank Network: The start from a German initiative. – Biopreservation and Biobanking 9: 51–55.

Gligora, M.; Kralj, K.; Plenković–Moraj, A.; Hinz, F.; Acs, E.; Grigorszky, I.; Cocquyt, C. & Van de Vijver, B.

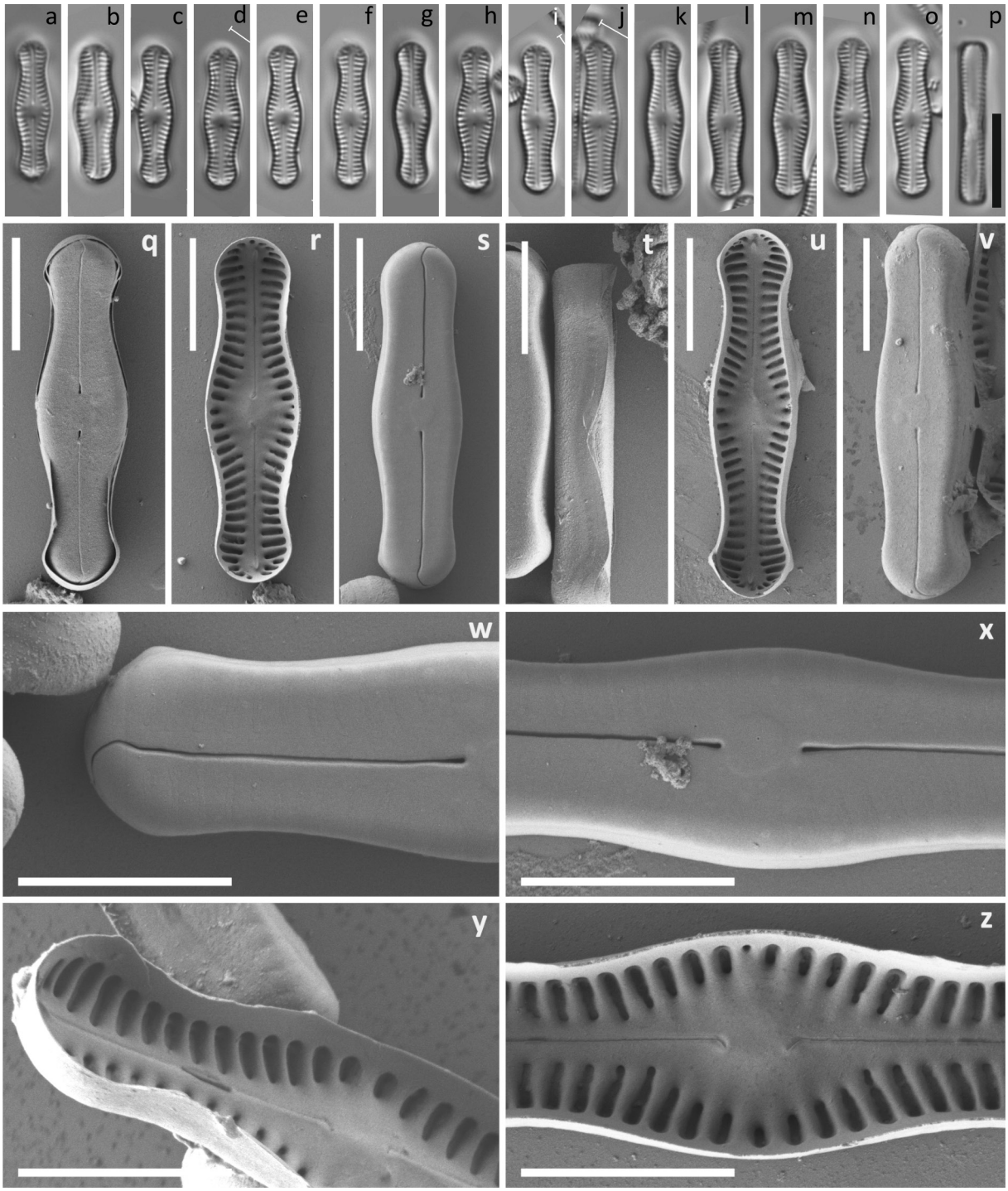

Fig. 6. *Chamaepinnularia krookii* LM and SEM: (a–p) LM pictures; (q–z) SEM pictures; (a–i, q–s, w–z) strain CCCryo 390–11; (j–p, t–v) strain CCCryo 443–14; (q, s, v, w, x) external view; (r, u, y, z) internal view; (w, x) external view with thick silicate hymen; (y, z) internal view on central area and striae with silicate bridges. Scale bars (a–p) 10 µm, (q–v) 5 µm, (w–z) 4 µm.

(2009): Observations on the diatom *Navicula hedinii* Hustedt (Bacillariophyceae) and its transfer to a new genus *Envekadea* Van de Vijver et al . gen. nov. – European Journal of Phycology 44: 123–138.

Goujon, M.; McWilliam, H.; Li, W.; Valentin, F.; Squizzato, S.; Paern, J. & Lopez, R. (2010): A new bioinformatics analysis tools framework at EMBL–EBI. – Nucleic Acids Research 38: W695–W699.

Grunow, A. (1882): Beiträge zur Kenntniss der Fossilen Diatomeen Österreich–Ungarns. – In: Mojsisovics, E. & Neumayr, N. (eds): Beiträge zur Paläontologie Österreich–Ungarns und des Orients. II Band Pt 4. – pp. 136–159, Alfred Hölder, Wien.

Gruenstaeudl, M. (2020): Annonex2embl: Automatic preparation of annotated DNA sequences for bulk submissions to ENA. – Bioinformatics 36: 3841–3848.

Guillard, R. R. & Ryther, J. H. (1962): Studies of marine planktonic diatoms: I. *Cyclotella nana* Hustedt, and *Detonula confervacea* (Cleve) Gran. – Canadian Journal of Microbiology 8: 229–239.

Guiry, M. D. & Guiry, G. M. (2022): AlgaeBase. – World–wide

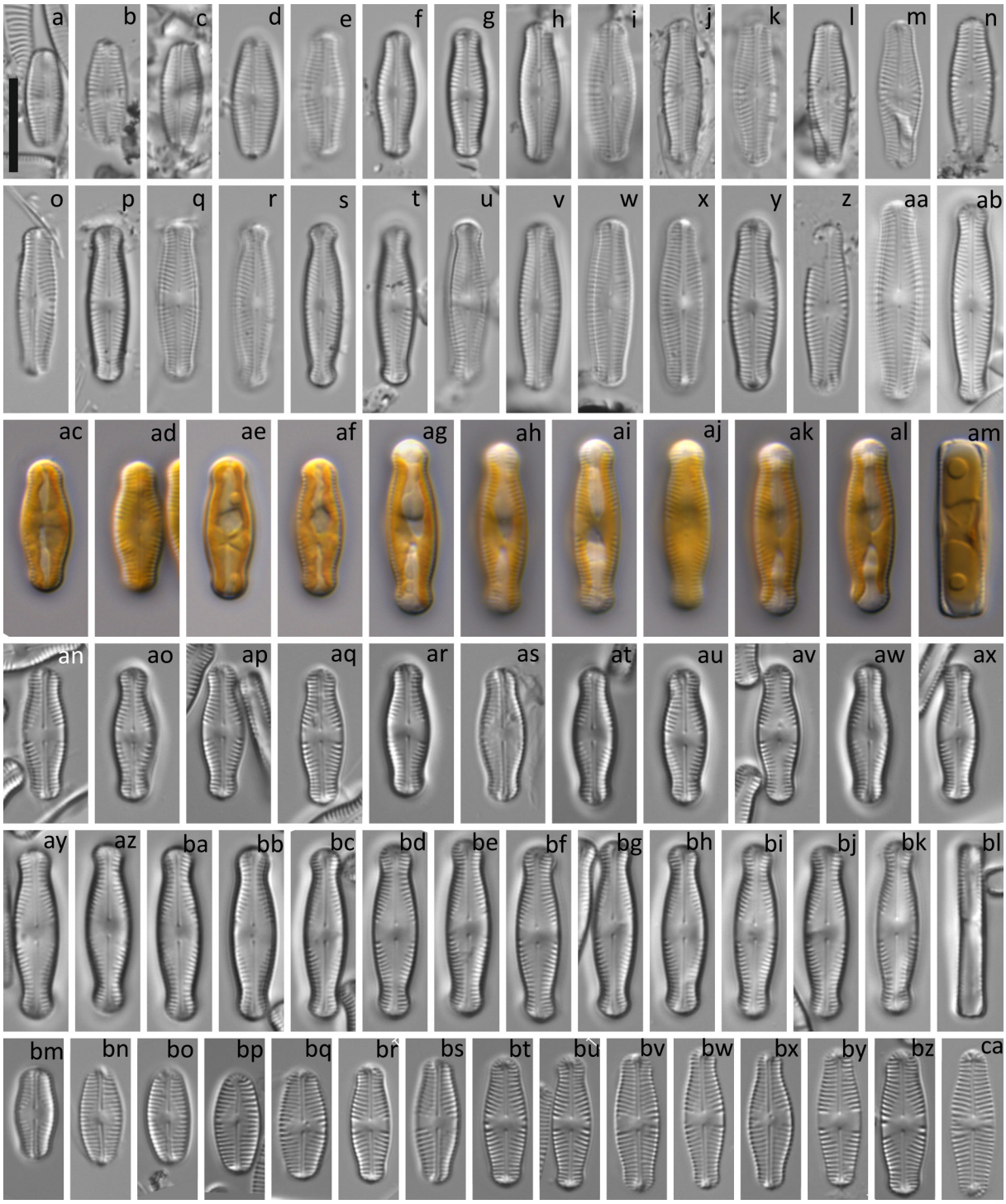

Fig. 7. *Chamaepinnularia australis* LM: (a–ab) valves from environmental sample; (ac–ca) valves from cultures; (ac–am) living cells with H–shaped plastid; (ac–af, an–ax) strain D294_013; (ag–aj, bc–bg) strain D294_001, bd represents the holotype; (ak–am, bh–bl) strain D294_002; (ay–bb) strain D294_014; (bm–ca) strain CCCryo 272–06. Scale bar 10 µm.

electronic publication. Available from https://www.algaebase.org/, accessed 07 Nov 2022.

JAHN, R.; ABARCA, N.; GEMEINHOLZER, B.; MORA, D.; SKIBBE, O.; KULIKOVSKIY, M.; GUSEV, E.; KUSBER, W.–H. & ZIMMERMANN, J. (2017): *Planothidium lanceolatum* and *Planothidium frequentissimum* reinvestigated with molecular methods and morphology: four new species and the taxonomic importance of the sinus and cavum. – Diatom Research 32: 75–107.

JAHN, R.; KUSBER, W.–H.; SKIBBE, O.; ZIMMERMANN, J.; VAN, A. T.; BUCZKÓ, K. & ABARCA, N. (2019): *Gomphonella olivacea* (Bacillariophyceae)–a new phylogenetic position for a well–known taxon, its typification, new species and combinations. – Plant Ecology and Evolution 152: 219–247.

KERMARREC L.; BOUCHEZ A.; RIMET F. & HUMBERT J.–F. (2013): First evidence of the existence of semi–cryptic species and of a phylogeographic structure in the *Gomphonema parvulum* (Kützing) Kützing complex (Bacillariophyta). – Protist 164: 686–705.

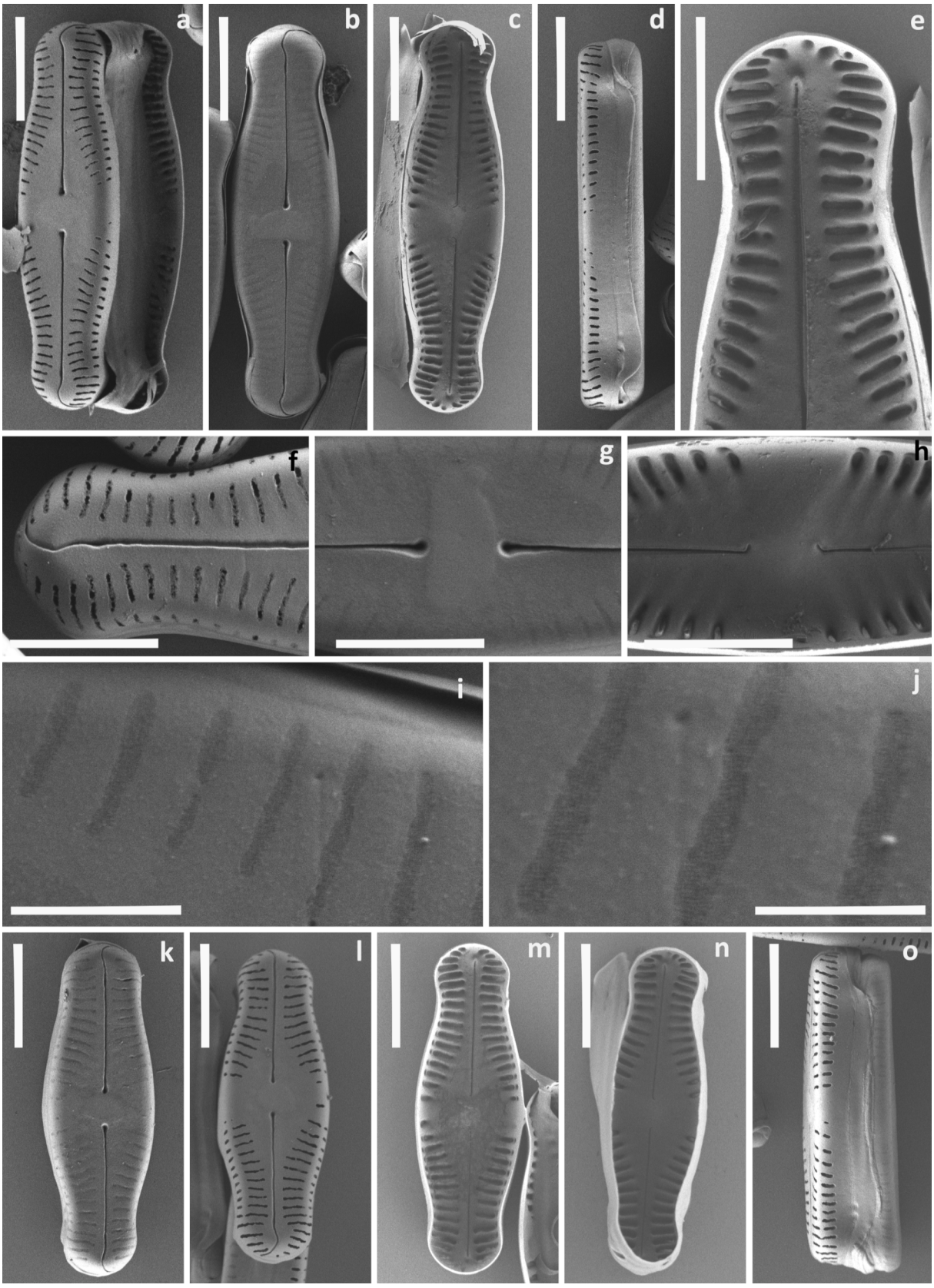

Fig. 8. *Chamaepinnularia australis* SEM1: (a–j) strain D294_001 (type strain); (k–o) strain D294_013; (a,b, f,g, i–l) external view; (c, e, h, m, n) internal view; (d, o) girdle view; (e) internal striae with silicate bridge and proximal raphe ending; (f) external striae separated by a hyaline line and corroded hymen; (g) external central area; (h) internal central area; (i–j) alveoli externally covered by hymen. Scale bars (a–d, k–o) 5 µm, (e–h) 3 µm, (i) 1 µm, (j) 0.5 µm.

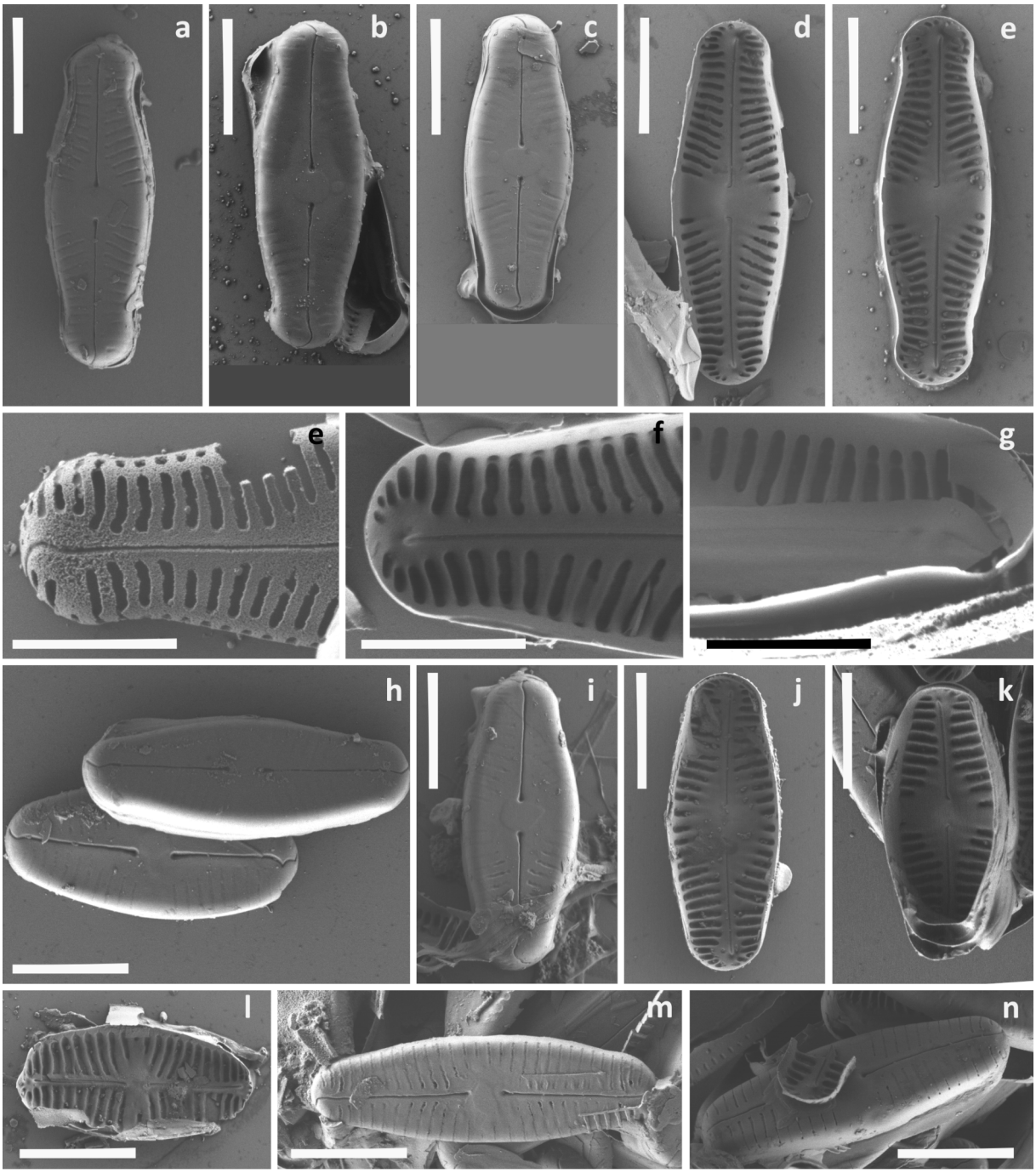

Fig. 9. *Chamaepinnularia australis* SEM2: (a–n) strain CCCryo 272–06, (a–c, h, i, m, n) external view; (d, e, j–l) internal view; (e) external striae separated by a hyaline line and completely corroded hymen; (f, g) internal striae with silicate bridge. Scale bars (a–d, h–n) 5 µm, (e–g) 3 µm.

KERMARREC, L.; FRANC, A.; RIMET, F.; CHAUMEIL, P.; FRIGERIO, J.–M.; HUMBERT, J.–F. & BOUCHEZ, A. (2014): A next–generation sequencing approach to river biomonitoring using benthic diatoms. – Freshwater Science 33: 349–363.

KEZLYA, E.; GLUSHCHENKO, A.; KOCIOLEK, J. P.; MALTSEV, Y.; MARTYNENKO, N.; GENKAL, S. & KULIKOVSKIY, M. (2020): *Mayamaea vietnamica* sp. nov.: a new, terrestrial diatom (Bacillariophyceae) species from Vietnam. – Algae 35: 325–335.

KOPALOVÁ, K.; VESELÁ, J.; ELSTER, J.; NEDBALOVÁ, L.; KOMÁREK, J. & VAN DE VIJVER, B. (2012): Benthic diatoms (Bacillariophyta) from seepages and streams on James Ross Island (NW Weddell Sea, Antarctica). – Plant Ecology and Evolution 145: 190–208.

KOCIOLEK, J. P.; STEPANEK, J. G.; LOWE, R. L.; JOHANSEN, J. R. & SHERWOOD, A. R. (2013): Molecular data show the enigmatic cave–dwelling diatom *Diprora* (Bacillariophyceae) to be a raphid diatom. – European Journal of Phycology 48: 474–484.

KRAMMER, K. (1992): *Pinnularia*. Eine Monographie der europäischen Taxa. – Bibliotheca Diatomologica 26. – 353 pp., J. Cramer, Berlin–Stuttgart.

KRAMMER, K. (2000): The genus *Pinnularia*. – In: LANGE–BERTALOT, H. (ed.): Diatoms of Europe 1. – 707 pp., A.R.G. Gantner Verlag K.G., Ruggell.

KULIKOVSKIY, M.; GLUSHCHENKO, A.; KUZNETSOVA, I. & KOCIOLEK, P. J. (2018): Description of the new freshwater diatom genus

Okhapkinia gen. nov. from Laos (Southeast Asia), with notes on family Sellaphoraceae Mereschkowsky 1902. – Fottea 18: 120–129.

Lange–Bertalot, H. (1997): *Frankophila, Mayamaea* und *Fistulifera*: drei neue Gattungen der Klasse Bacillariophyceae. – Archiv für Protistenkunde 148: 65–76.

Lange–Bertalot, H. & Genkal, S. I. (1999): Diatomeen aus Sibirien, I: Inseln im Arktischen Ozean (Yugorsky – Shar Strait) / Diatoms from Siberia, I: Islands in the Arctic Ocean (Yugorsky – Shar Strait). – Iconographia Diatomologica 6: 1–292.

Lange–Bertalot, H. & Metzeltin, D. (1996): Indicator of Oligotrophy. 800 taxa representative of three ecologically distinct lake types, carbonate buffered–Oligodystrophic–weakly buffered soft water. – Iconographia Diatomologica 2: 1–390.

Li, Y.; Suzuki, H.; Nagumo, T.; Tanaka, J.; Sun, Z. & Xu, K. (2022): Morphology, molecular phylogeny and systematics of the diatom genus *Fallacia* (Sellaphoraceae), with descriptions of three new species. – Journal of Phycology 58: 449–464.

Liu, Y.; Kociolek, J. P.; Fan, Y. & Wang, Q. (2012): *Pseudofallacia* gen. nov., a new freshwater diatom (Bacillariophyceae) genus based on *Navicula occulta* Krasske. – Phycologia 51: 620–626.

Main, S.P. (2003): *Diprora haenaensis* gen. et sp. nov. a filamentous, pseudoaerial, araphid diatom from Kaua'I (Hawaiian Islands). – Diatom Research 18: 259–272.

Maltsev, Y.; Andreeva, S.; Kulikovskiy, M.; Podunay, Y. & Kociolek, P. (2017): Molecular phylogeny of the diatom genus *Envekadea* (Bacillariophyceae, Naviculales). – Nova Hedwigia 146 146: 241–252.

Mann, D.G. (1989): The diatom genus *Sellaphora*: Separation from *Navicula*. – British Phycological Journal 24: 1–20.

Metzeltin, D.; Lange–Bertalot, H. & Nergui, S. (2009): Diatoms in Mongolia. – Iconographia Diatomologica 20: 691 pp.

Mereschkowsky, C. (1902): On *Sellaphora*, a new genus of diatoms. – Journal of Natural history 9: 185–195.

Miller, M.A.; Pfeiffer, W. & Schwartz, T. (2010): Creating the CIPRES Science Gateway for inference of large phylogenetic trees. – 2010 Gateway Computing Environments Workshop (GCE) 1–8.

Mohamad, H.; Mora, D.; Skibbe, O.; Abarca, N.; Deutschmeyer, V.; Enke, N.; Kusber, W.–H.; Zimmermann, J. & Jahn, R. (2022): Morphological and genetic stability of monoclonal diatom strains during a two–year period. – Diatom Research 37: 307–328.

Mora, D.; Abarca, N.; Proft, S.; Grau, J.H.; Enke, N.; Carmona, J.; Skibbe, O.; Jahn, R. & Zimmermann, J. (2019): Morphology and metabarcoding: a test with stream diatoms from Mexico highlights the complementarity of identification methods. – Freshwater Science 38: 448–464.

Müller, J.; Müller, K.; Neinhuis, C. & Quandt, D. (2010): PhyDE®–Phylogenetic Data Editor version 0.9971. http://www.phyde.de.

Nakov, T.; Beaulieu, J.M. & Alverson, A.J. (2018): Accelerated diversification is related to life history and locomotion in a hyperdiverse lineage of microbial eukaryotes (Diatoms, Bacillariophyta). – New Phytologist 219: 462–473.

Pérez–Burillo, J.; Valoti, G.; Witkowski, A.; Prado, P.; Mann, D. G. & Trobajo, R: (2022): Assessment of marine benthic diatom communities: insights from a combined morphological–metabarcoding approach in Mediterranean shallow coastal waters. – Marine Pollution Bulletin 174: 113183.

PhycoBank (2017+): Registration of Nomenclatural Acts of Algae. Available from https://phycobank.org, accessed 07 Nov 2022.

Pinseel, E; Jansens, S. B.; Verleyen, E.; Vanormelingen, P.; Kohler, T.J.; Biersma, E.M.; Sabbe, K.; Van de Vijver, B. & Vyverman, W. (2020): Global radiation in a rare biosphere soil diatom. – Nature Communications 11: 2382.

Potapova, M. (2014): Diatoms of Bering Island, Kamchatka, Russia. Nova Hedwigia, Beiheft: 63–102.

Poulin, M. (1993): *Craspedopleura* (Bacillariophyta), a new diatom genus of arctic sea ice assemblages. – Phycologia 32: 223–233.

Prelle, L.R.; Schmidt, I.; Schimani, K.; Zimmermann, J.; Abarca, N.; Skibbe, O.; Juchem, D. & Karsten, U. (2022): Photosynthetic, Respirational, and Growth Responses of Six Benthic Diatoms from the Antarctic Peninsula as Functions of Salinity and Temperature Variations. – Genes 13: 1264.

Rambaut, A. (2009): FigTree version 1.4.4.

Rambaut, A.; Drummond, A.J.; Xie, D.; Baele, G. & Suchard, M. A. (2018): Tracer v1.7. Available from http://beast.community/tracer.

Ronquist, F.; Teslenko, M.; Mark, P.; Ayres, D.; Darling, A.; Höhna, S.; Larget, B.; Liu, L.; Suchard, M. & Huelsenbeck, J. (2012): MrBayes 3.2: Efficient Bayesian Phylogenetic Inference and Model Choice Across a Large Model Space. – Systematic biology 61: 539–42.

Round, F.E.; Crawford, R.M. & Mann, D.G. (1990): Diatoms: biology and morphology of the genera. – 747 pp., Cambridge University Press, Cambridge.

Sabbe, K.; Vyverman, W. & Muylaert, K. (1999): New and little–known *Fallacia* species (Bacillariophyta) from brackish and marine intertidal sandy sediments in Northwest Europe and North America. – Phycologia 38: 8–22.

Silva, J.F.; Oliveira, M.A.; Alves, R.P.; Cassol, A.P.V.; Anunciação, R.R.; Silva, E.P.; Schünemann, A.L. & Pereira, A.B. (2019): Geographic distribution of epilithic diatoms (Bacillariophyceae) in Antarctic lakes, South Shetland Islands, Maritime Antarctica Region. – Check List 15: 797–809.

Souffreau, C.; Verbruggen, H.; Wolfe, A.P.; Vanormelingen, P.; Siver, P.A.; Cox, E.J.; Mann, D.G.; Van de Vijver, B.; Sabbe, K. & Vyverman, W. (2011): A time–calibrated multi–gene phylogeny of the diatom genus *Pinnularia*. – Molecular Phylogenetics and Evolution 61: 866–79.

Spijkerman, E.; Wacker, A.; Weithoff, G. & Leya, T. (2012): Elemental and fatty acid composition of snow algae in Arctic habitats. – Fronters in Microbiology 3: 380.

Stamatakis, A. (2014): RAxML version 8: a tool for phylogenetic analysis and post–analysis of large phylogenies. – Bioinformatics 30: 1312–1313.

Stamatakis, A.; Hoover, P. & Rougemont, J. (2008): A Rapid Bootstrap Algorithm for the RAxML Web Servers. – Systematic Biology 57: 758–771.

Sterken, M.; Verleyen, E.; Jones, V.; Hodgson, D.; Vyverman, W.; Sabbe, K. & Van de Vijver, B. (2015): An illustrated and annotated checklist of freshwater diatoms (Bacillariophyta) from Livingston, Signy and Beak Island (Maritime Antarctic Region). – Plant Ecology and Evolution 148: 431–455.

Su, Y.; Lundholm, N. & Ellegaard, M. (2018): Effects of abiotic factors on the nanostructure of diatom frustules—ranges and variability. – Applied Microbiology and Biotechnology: 102, 5889–5899.

Tamura, K.; Stecher, G. & Kumar, S. (2021): MEGA11: Molecular Evolutionary Genetics Analysis Version 11. – Molecular Biology and Evolution 38: 3022–3027.

Turland, N.J.; Wiersema, J.H.; Barrie, F.R.; Greuter, W.; Hawksworth, D.L.; Herendeen, P.S.; Knapp, S.; Kusber, W.–H.; Li, D.–Z.; Marhold, K.; May, T.W.; McNeill, J.; Monro, A.M.; Prado, J.; Price, M.J. & Smith, G.F. (2018): International Code of Nomenclature for algae, fungi, and plants (Shenzhen Code) adopted by the Nineteenth International Botanical Congress Shenzhen, China, July 2017. Glashütten: Koeltz Botanical Books.

Van de Vijver, B.; Beyens, L.; Vincke, S. & Gremmen, N. (2004): Moss–inhabiting diatom communities from Heard Island, sub–Antarctic. – Polar Biology 27:532–543.

Van de Vijver, B. & Cox, E.J. (2013): New and interesting small–celled naviculoid diatoms (Bacillariophyceae) from a lava tube cave on Île Amsterdam (TAAF, Southern Indian Ocean)

– Cryptogamie, Algologie 34: 37–47.
VAN DE VIJVER, B.; FRENOT, Y. & BEYENS, L. (2002): Freshwater diatoms from Ile de la Possession (Crozet Archipelago, Subantarctica). – 412 pp., Cramer, Berlin.
VAN DE VIJVER, B.; KOPALOVÁ, K.; ZIDAROVA, R. & COX, E. (2013): New and interesting small–celled naviculoid diatoms (Bacillariophyta) from the Maritime Antarctic Region. – Nova Hedwigia 97: 189–208.
VAN DE VIJVER, B.; STERKEN, M.; VYVERMAN, W.; MATALONI, G.; NEDBALOVÁ, L.; KOPALOVÁ, K.; ELSTER, J.; VERLEYEN, E. & SABBE, K. (2010): Four new non–marine diatom taxa from the Subantarctic and Antarctic regions. – Diatom Research 25: 431–443.
VAN DE VIJVER, B.; TAVERNIER, I.; KELLOGG, T. B.; GIBSON, J.; VERLEYEN, E.; VYVERMAN, W. & SABBE, K. (2012): Revision of type materials of Antarctic diatom species (Bacillariophyta) described by West & West (1911), with the description of two new species. – Fottea 12: 149–169.
VASSELON, V.; RIMET, F.; TAPOLCZAI, K. & BOUCHEZ, A. (2017): Assessing ecological status with diatoms DNA metabarcoding: Scaling–up on a WFD monitoring network (Mayotte island, France). – Ecological Indicators 82: 1–12.
VERLEYEN, E.; VAN DE VIJVER, B.; TYTGAT, B.; PINSEEL, E.; HODGSON, D.A.; KOPALOVÁ, K.; CHOWN, S. L.; VAN RANST, E.; IMURA, S.; KUDOH, S.; VAN NIEUWENHUYZE, W.; SABBE, K. & VYVERMAN, W. (2021): Diatoms define a novel freshwater biogeography of the Antarctic. – Ecography 44: 548–560.
VISCO, J. A.; APOTHÉLOZ–PERRET–GENTIL, L.; CORDONIER, A.; ESLING, P.; PILLET, L. & PAWLOWSKI, J. (2015): Environmental Monitoring: Inferring the Diatom Index from Next–Generation Sequencing Data. – Environmental Science & Technology 49: 7597–7605.
VYVERMAN, W.; VERLEYEN, E.; WILMOTTE, A.; HODGSON, D.A.; WILLEMS, A.; PEETERS, K.; VAN DE VIJVER, B.; DE WEVER, A.; LELIAERT, F. & SABBE, K. (2010): Evidence for widespread endemism among Antarctic micro–organisms. – Polar Science 4: 103–113.
WERUM, M. & LANGE–BERTALOT, H. (2004): Diatoms in Springs. rom Central Europe and elsewhere under the influence of hydrogeology and anthropogenic impages. – Iconographia Diatomologica 13: 1–417.
WETZEL, C.E. & ECTOR, L. (2016): On the identity of *Chamaepinnularia thermophila* comb. nov. (Bacillariophyceae) from a Neotropical thermal spring. – Phytotaxa 260: 95–97.
WETZEL, C.E.; ECTOR, L.; VAN DE VIJVER, B.; COMPÈRE, P. & MANN, D.G. (2015): Morphology, typification and critical analysis of some ecologically important small naviculoid species (Bacillariophyta). – Fottea 15: 203–234.
WETZEL, C.E.; MARTÍNEZ–CARRERAS, N.; HLÚBIKOVÁ, D.; HOFFMANN, L.; PFISTER, L. & ECTOR, L. (2013): New Combinations and Type Analysis of *Chamaepinnularia* species (Bacillariophyceae) from Aerial Habitats. – Cryptogamie Algologie 34: 149–168.
WITKOWSKI, A.; LANGE–BERTALOT, H. & METZELTIN, D. (2000): Diatom Flora of Marine Coasts I. – 925 pp., Koeltz Scientific Books, Königstein.
YANA, E.; NAKKAEW, S.; PEKKOH, J.; PEERAPORNPISAL, Y.; TUJI, A.; DAVIS, M.P.; JULIUS, M.L. & MAYAMA, S. (2022): Valve and 'Stigma' Structure and Phylogeny of an Enigmatic Cymbelloid Diatom *Karthickia verestigmata* Glushchenko, Kulikovskiy & Kociolek. – Diatom Research 37: 293–305.
ZACHER, K.; RAUTENBERGER, R.; DIETER, H.; WULFF, A. & WIENCKE, C. (2009): The abiotic environment of polar marine benthic algae. – Botanica Marina 52: 483–490.
ŻELAZNA–WIECZOREK, J. & OLSZYŃSKI, M.R. (2016): Taxonomic revision of *Chamaepinnularia krookiformis* Lange–Bertalot et Krammer with a description of *Chamaepinnularia plinskii* sp. nov. – Fottea 16: 112–121.
ZIDAROVA, R.; KOPALOVÁ, K. & VAN DE VIJVER, B. (2016a): Ten new Bacillariophyta species from James Ross Island and the South Shetland Islands (Maritime Antarctic Region). – Phytotaxa 272: 37–62.
ZIDAROVA, R.; KOPALOVÁ, K. & VAN DE VIJVER, B. (2016b): Diatoms from the Antarctic Region. I: Maritime Antarctica. – 504 pp., Koeltz Botanical Books, Schmitten - Oberreifenberg.
ZIMMERMANN, J.; JAHN, R. & GEMEINHOLZER, B. (2011): Barcoding diatoms: evaluation of the V4 subregion on the 18S rRNA gene, including new primers and protocols. – Organisms Diversity & Evolution 11: 173.
ZIMMERMANN, J.; GLÖCKNER, G.; JAHN, R.; ENKE, N. & GEMEINHOLZER, B. (2015): Metabarcoding vs. morphological identification to assess diatom diversity in environmental studies. – Molecular Ecology Resources 15: 526–542.

Supplementary material

The following supplementary material is available for this article:

Supplementary Material 1. Freshwater and brackish water culture medium recipes used by the Culture Collection of Cryophilic Algae.

Supplementary Material 2. List of taxa included obtained from GenBank for this study with strain name, taxon name, accession number 18S and rbcL as well as reference, where the sequence was published.

Supplementary Material 3. 18S rRNA gene alignment without the hypervariate part of the V4 region of *Chamaepinnularia* species and sequences obtained from GenBank.

Supplementary Material 4. rbcL gene alignment of *Chamaepinnularia* species and sequences obtained from GenBank.

Supplementary Material 5. Maximum likelihood (ML) and Bayesian inference (BI) phylogenetic tree based on the 18S rRNA gene. Nodal support for branches in the ML and BI trees is marked in order (ML/BI). Only bootstrap values over 70% and posterior probability over 96% are shown in the tree.

Supplementary Material 6. Maximum likelihood (ML) and Bayesian inference (BI) phylogenetic tree based on the *rbc*L gene. Nodal support for branches in the ML and BI trees is marked in order (ML/BI). Only bootstrap values over 70% and posterior probability over 96% are shown in the tree.

Supplementary Material 7. Maximum likelihood (ML) phylogenetic tree based on the concatenated 18S rRNA and rbcL gene sequences with all strains including incomplete or shorter sequences. Only bootstrap values over 70% are shown in the tree.

Supplementary Material 8. Percent dissimilarity (p–distance) matrix of 12 *Chamaepinnularia* strains on basis of the 18S rRNA gene including the V4 subregion (1543 bp), on basis of the barcode of the V4 region of the 18S rRNA commonly used in diatom DNA metabarcoding (282 bp) and percent dissimilarity (p–distance) matrix of 12 *Chamaepinnularia* strains on basis of the rbcL gene (990 bp) on basis of the barcode of the rbcL gene commonly used in diatom DNA metabarcoding (263 bp).

This material is available as part of the online article (http://fottea.czechphycology.cz/contents)

Received November 17, 2022
Accepted January 16, 2023